



Fourth order energy-preserving locally implicit time discretization for linear wave equations

Juliette Chabassier, Sébastien Imperiale

► To cite this version:

Juliette Chabassier, Sébastien Imperiale. Fourth order energy-preserving locally implicit time discretization for linear wave equations. International Journal for Numerical Methods in Engineering, 2015, 10.1002/nme.5130 . hal-01222072

HAL Id: hal-01222072

<https://inria.hal.science/hal-01222072>

Submitted on 29 Oct 2015

HAL is a multi-disciplinary open access archive for the deposit and dissemination of scientific research documents, whether they are published or not. The documents may come from teaching and research institutions in France or abroad, or from public or private research centers.

L'archive ouverte pluridisciplinaire **HAL**, est destinée au dépôt et à la diffusion de documents scientifiques de niveau recherche, publiés ou non, émanant des établissements d'enseignement et de recherche français ou étrangers, des laboratoires publics ou privés.

Fourth order energy-preserving locally implicit time discretization for linear wave equations

J. Chabassier¹, S. Imperiale^{2*}

¹ *Magique-3D Team, Inria Bordeaux Sud Ouest - University of Pau and Pays de l'Adour, Pau, France.*

² *M3DISIM Team, Inria Saclay, Palaiseau, France.*

SUMMARY

A family of fourth order coupled implicit-explicit time schemes is presented as a special case of fourth order coupled implicit schemes for linear wave equations. The domain of interest is decomposed into several regions where different fourth order time discretization are used, chosen among a family of implicit or explicit fourth order schemes. The coupling is based on a Lagrangian formulation on the boundaries between the several non conforming meshes of the regions. A global discrete energy is shown to be preserved and leads to global fourth order consistency in time. Numerical results in 1d and 2d for the acoustic and elastodynamics equations illustrate the good behavior of the schemes and their potential for the simulation of realistic highly heterogeneous media or strongly refined geometries, for which using everywhere an explicit scheme can be extremely penalizing. Accuracy up to fourth order reduces the numerical dispersion inherent to implicit methods used with a large time step, and makes this family of schemes attractive compared to second order accurate methods.

KEY WORDS: Wave equations, High-order numerical methods, Time discretization, Locally implicit schemes, Consistency analysis.

1. INTRODUCTION

Numerous transient physical phenomena can be modeled by linear wave equations, as for instance Maxwell's equations for electromagnetism, the acoustic equation for the sound propagation and the elastodynamic equation for the propagation of waves in solids. Their solution in realistic media and geometries can be approximated by direct numerical simulations. Efficient numerical methods are now available to discretize this kind of problems in space and time. Among them, the finite elements method [1] for space discretization combined with energy-preserving explicit methods based on a constant time step Δt for time discretization (as the leap-frog scheme [2]) gather various advantages since it can follow complex geometries in any dimension, achieve high order of accuracy in space and guarantee important mathematical properties as energy preservation. Specific choices of numerical integration can lead to a diagonal mass matrix, also called "mass lumping technique" [2, 3, 4], which drastically reduces the computational cost for explicit time schemes and ensures high order of accuracy in space. Energy identities provide proofs of stability under a constraint on the time step (the so called CFL condition). A stable coupling of these methods in different dimensions or regions of space, or for different wave equations is also done in a stable way via energy estimations and more specifically using Lagrange multipliers, see [5] for modeling the propagation of waves in a guitar. These numerical techniques provide a very efficient approach in most application cases. However, the upper bound on the time step can prove too restrictive in

*Correspondence to: sebastien.imperiale@inria.fr

specific configurations.

For scattering problems for instance, or more generally for problems where the heterogeneities are localized in space, a local treatment in space is desirable using standard (h/p) refinement processes. A coarse mesh is used everywhere, and is refined in space or order near the obstacle or the complex geometry. Other cases arise in which a localized region have a high velocity of propagation. In such situations, the standard explicit time discretization is not optimal since the time step must indeed be adapted to the worst situation (for instance the smallest element or the highest velocity, or a combination of both) because of the CFL condition. A natural way to avoid this rather common efficiency loss is to use local time stepping techniques. The development of local time stepping schemes for hyperbolic systems is a vivid research field, these schemes are based upon Runge-Kutta schemes ([6, 7]) or “Arbitrary high order derivatives” (ADER) time discretization ([8, 9, 10]). It is not straightforward to extend the previous mentioned work to second order energy preserving wave propagation problems, therefore appropriate methods have been developed, they fall into two categories:

- The implicit local time-stepping technique, as developed in [11, 12], and [13], is optimal in term of CFL restriction but “only” second order accurate in time, and requires the inversion of interface matrices.
- The fully explicit local time stepping, as developed in [14], achieves higher order time stepping but without (up to now) a full control over the CFL condition.

Another alternative to high order conservative explicit time stepping is developed in [15], which consists in a family of accurate (fourth order in time) implicit schemes, depending on two real parameters θ and φ . These schemes are stable under a relaxed (or sometimes inexistent) stability condition that depends on the chosen parameters’ values. However, using such a scheme in the whole computational domain requires the inversion of a global linear system, which seems a dramatic over cost compared to the local nature of the tackled difficulty. Therefore a natural idea is to develop a locally implicit fourth-order time discretization in which an explicit scheme is solved in the non constraining part of the domain (which imposes the value of Δt) and implicit schemes are solved locally in the constraining regions of the domain. Specific choices of the parameters θ and φ allow that the same time step Δt is used for all the regions of the mesh and leads to a stable discretization. This is the objective of this article. A first specificity arises from the coupling in space: we will choose to use mortar element technique [3] so that non conforming meshes can be used. The major difficulty will be to ensure stability while guarantying a global fourth order consistency in time. Similar approaches exist for second order accuracy in time for conformal spatial discretization [16, 17, 18] for Maxwell’s equations using Discontinuous Galerkin methods).

In the following, and for the sake of simplicity, we restrict ourselves to the second order scalar wave equation. The proposed time discretization can however be applied to other conservative second order wave propagation systems such as elastodynamic equations (see the numerical illustration in Figure 10), beams and plates’ equations or Maxwell’s equations.

In section 2, we reformulate the continuous scalar acoustic equation stated in the whole domain as a transmission problem across an artificial boundary which materializes the transition between two regions. At the boundary, a new unknown is introduced and stands as a Lagrange multiplier expressing the continuity of the flux between the two regions. The generalization to more regions follows easily from this simple configuration. We then provide a semi discretization in space of this transmission problem. The time discretization is the object of the following sections and we proceed in a progressive manner. As the explicit-implicit coupling is a special case of coupled implicit coupling (or implicit-implicit coupling), we consider this latter case for more generality and call it “hybrid schemes”. In section 3, we first pedagogically introduce our technical approach in a rather simple context (classical implicit second-order schemes), in view of using the same approach for coupling fourth-order implicit schemes. We present hybrid second-order time schemes where classical second-order implicit schemes are coupled together. A practical solution algorithm

is provided, followed by proofs of global stability and accuracy via energy techniques. In section 4, the same approach is followed in order to construct hybrid schemes based on the family of fourth-order implicit schemes developed in [15], and we prove them stable and fourth-order accurate. This theoretical convergence result is then illustrated with numerical experiments. Two-dimensional simulation cases are performed in order to show the efficiency of these hybrid schemes for highly heterogeneous situations.

2. LAGRANGIAN BASED SEMI-DISCRETE FORMULATION

This section is devoted to the reformulation of the wave problem into a transmission problem, followed by its discretization in space.

2.1. Artificial decomposition of the domain

We want to solve for time $t > 0$, the following equation:

$$\begin{cases} \partial_t^2 u - \nabla \cdot c^2(\mathbf{x}) \nabla u = s & \text{in } \Omega \\ \nabla u \cdot \mathbf{n} = 0 & \text{on } \partial\Omega \end{cases} \quad (1a)$$

$$(1b)$$

in a domain Ω , where s is a given source term, \mathbf{n} the outward normal to the boundary and $c(\mathbf{x}) > c_0 > 0$ the inhomogeneous velocity of the waves. The variational formulation of (1) reads

$$\begin{cases} \text{Find } u(t) \in H^1(\Omega), \text{ such that } \forall v \in H^1(\Omega), \\ \int_{\Omega} \partial_t^2 u v + \int_{\Omega} c^2(\mathbf{x}) \nabla u \cdot \nabla v = \int_{\Omega} s v \end{cases} \quad (2a)$$

$$(2b)$$

Taking as test function $\partial_t u$, it is standard to show that any solution to (2) satisfies the energy identity

$$\frac{d\mathcal{E}}{dt} = \int_{\Omega} s \partial_t u, \text{ where } \mathcal{E} = \frac{1}{2} \|\partial_t u\|_{L^2(\Omega)}^2 + \frac{1}{2} \|c \nabla u\|_{L^2(\Omega)}^2 \quad (3)$$

Our continuous problem (1) is also strictly equivalent to the following transmission problem, where we artificially decomposed the domain into disjoint sets $\Omega = \Omega_0 \cup \Omega_1$ and we denote $\Gamma = \overline{\Omega_0} \cap \overline{\Omega_1}$:

$$\begin{cases} \text{Find } u_0(t) \in H^1(\Omega_0), u_1(t) \in H^1(\Omega_1) \text{ and } \lambda(t) \in H^{-1/2}(\Gamma) \text{ such that} \\ \forall v_0 \in H^1(\Omega_0), \forall v_1 \in H^1(\Omega_1) \text{ and } \phi \in H^{-1/2}(\Gamma), \end{cases} \quad (4a)$$

$$\int_{\Omega_0} \partial_t^2 u_0 v_0 + \int_{\Omega_0} c^2(\mathbf{x}) \nabla u_0 \cdot \nabla v_0 = \int_{\Omega_0} s_0 v_0 + \int_{\Gamma} \lambda v_0 \quad (4b)$$

$$\int_{\Omega_1} \partial_t^2 u_1 v_1 + \int_{\Omega_1} c^2(\mathbf{x}) \nabla u_1 \cdot \nabla v_1 = \int_{\Omega_1} s_1 v_1 - \int_{\Gamma} \lambda v_1 \quad (4c)$$

$$\int_{\Gamma} u_0 \phi = \int_{\Gamma} u_1 \phi \quad (4d)$$

Notice that an artificial unknown λ appears in order to balance the constraint (4d) on the artificial boundary Γ . If we reinterpret this variational formulation in its strong form, we understand that λ is the Lagrange multiplier associated to the condition of continuity of the flux across Γ :

$$\begin{cases} \partial_t^2 u_0 - \nabla \cdot c^2(\mathbf{x}) \nabla u_0 = s_0 & \text{in } \Omega_0, & \partial_t^2 u_1 - \nabla \cdot c^2(\mathbf{x}) \nabla u_1 = s_1 & \text{in } \Omega_1, \end{cases} \quad (5a)$$

$$\begin{cases} c^2(\mathbf{x}) \nabla u_0 \cdot \mathbf{n}_0 = \lambda & \text{on } \Gamma, & c^2(\mathbf{x}) \nabla u_1 \cdot \mathbf{n}_1 = -\lambda & \text{on } \Gamma, \end{cases} \quad (5b)$$

$$u_0 = u_1 \quad \text{on } \Gamma \quad (5c)$$

Where \mathbf{n}_0 is the outward normal to Γ from Ω_0 and $\mathbf{n}_0 = -\mathbf{n}_1$. The energy associated to (4) is obtained by taking as test functions : $v_0 = \partial_t u_0$, $v_1 = \partial_t u_1$, $\phi = \lambda$. Differentiating (4d) with respect

to time, we see that the contributions due to the Lagrange multiplier λ cancel out and we get:

$$\begin{aligned} \frac{d\mathcal{E}_{01}}{dt} &= \int_{\Omega_0} s_0 \partial_t u_0 + \int_{\Omega_1} s_1 \partial_t u_1, \text{ where} \\ \mathcal{E}_{01} &= \frac{1}{2} \|\partial_t u_0\|_{L^2(\Omega_0)}^2 + \frac{1}{2} \|\partial_t u_1\|_{L^2(\Omega_1)}^2 + \frac{1}{2} \|c \nabla u_0\|_{L^2(\Omega_0)}^2 + \frac{1}{2} \|c \nabla u_1\|_{L^2(\Omega_1)}^2 \end{aligned} \quad (6)$$

Remark 2.1

Notice that this energy is the same as (3), i.e. $\mathcal{E}_{01} = \mathcal{E}$, since u is an H^1 function and can be constructed from u_0 and u_1 which are simply its restrictions on Ω_0 and Ω_1 .

2.2. Semi discretization in space

In the following, we will abusively use the notation $\|X\|_M^2 = MX \cdot X$ for any symmetric matrix M and vector X (with M non necessarily definite positive).

Let us consider a finite element discretization in space on meshes of Ω_0 and Ω_1 as well as finite dimensional finite element space based upon these meshes: $\mathcal{V}_{h,0} \subset H^1(\Omega_0)$, $\mathcal{V}_{h,1} \subset H^1(\Omega_1)$ and $\Gamma_h \subset H^{-1/2}(\Gamma)$. Note that it is also possible to use non-conforming methods, among them the Interior Penalty Discontinuous Galerkin method (IPDG, see [19]) gives a semi-discrete scheme compatible with the fully discrete schemes presented in what follows.

One has leeway in the choice of $(\mathcal{V}_{h,0}, \mathcal{V}_{h,1})$ after which Γ_h can not be chosen arbitrarily since an inf-sup type condition must be satisfied, see [13, 20, 21], for more details. After having constructed the semi-discrete matrix formulation of the problem, we define $(\tilde{U}_{h,0}, \tilde{U}_{h,1}, \tilde{\Lambda}_h)$ as the semi discrete solution of:

$$\begin{cases} d_t^2 M_{h,0} \tilde{U}_{h,0} + K_{h,0} \tilde{U}_{h,0} - {}^t C_{h,0} \tilde{\Lambda}_h = M_{h,0} \tilde{S}_{h,0} & (7a) \\ d_t^2 M_{h,1} \tilde{U}_{h,1} + K_{h,1} \tilde{U}_{h,1} + {}^t C_{h,1} \tilde{\Lambda}_h = M_{h,1} \tilde{S}_{h,1} & (7b) \\ C_{h,0} \tilde{U}_{h,0} = C_{h,1} \tilde{U}_{h,1} & (7c) \end{cases}$$

where the mass matrices $M_{h,0}$ and $M_{h,1}$ are positive symmetric matrices and the stiffness matrices $K_{h,0}$ and $K_{h,1}$ are symmetric non-negative. Multiplying (7a) by $d_t \tilde{U}_{h,0}$ and (7b) by $d_t \tilde{U}_{h,1}$, and differentiating (7c) with respect to time, we get the following semi-discrete energy identity:

$$\begin{aligned} \frac{d\mathcal{E}_{01,h}}{dt} &= M_{h,0} \tilde{S}_{h,0} \cdot d_t \tilde{U}_{h,0} + M_{h,1} \tilde{S}_{h,1} \cdot d_t \tilde{U}_{h,1} \quad \text{where} \\ \mathcal{E}_{01,h} &= \frac{1}{2} \|d_t \tilde{U}_{h,0}\|_{M_{h,0}}^2 + \frac{1}{2} \|d_t \tilde{U}_{h,1}\|_{M_{h,1}}^2 + \frac{1}{2} \|\tilde{U}_{h,0}\|_{K_{h,0}}^2 + \frac{1}{2} \|\tilde{U}_{h,1}\|_{K_{h,1}}^2 \end{aligned} \quad (8)$$

Remark 2.2

Up to now we have not specified any algebraic property for the rectangular matrices $C_{h,0}$ and $C_{h,1}$. By multiplying (7a) by $M_{h,0}^{-1}$ then by $C_{h,0}$, doing the same for (7b) we get, after subtraction and using (7c):

$$\begin{aligned} \left[C_{h,0} M_{h,0}^{-1} {}^t C_{h,0} + C_{h,1} M_{h,1}^{-1} {}^t C_{h,1} \right] \tilde{\Lambda}_h(t^n) = \\ C_{h,0} M_{h,0}^{-1} K_{h,0} \tilde{U}_{h,0}(t^n) - C_{h,0} \tilde{S}_{h,0} - C_{h,1} M_{h,1}^{-1} K_{h,1} \tilde{U}_{h,1}(t^n) + C_{h,1} \tilde{S}_{h,1}. \end{aligned} \quad (9)$$

The existence of a unique $\tilde{\Lambda}_h(t^n)$ is a consequence of the invertibility of $C_{h,0} M_{h,0}^{-1} {}^t C_{h,0} + C_{h,1} M_{h,1}^{-1} {}^t C_{h,1}$. The existence of an inverse is guaranteed by a discrete inf-sup condition (see [13, 22]), in our case the condition is equivalent to

$$\ker C_{h,0} \cap \ker C_{h,1} = \{0\}. \quad (10)$$

In the simple case of one interface, a systematic approach can be implemented to ensure that the previous equality is true, it consists in choosing Γ_h as the trace-space of either $\mathcal{V}_{h,1}$ or $\mathcal{V}_{h,2}$.

3. SECOND ORDER CONSERVATIVE HYBRID SCHEMES

One of the main features of the schemes that we want to derive is that the time step is constant and the same in all the domain. We denote this time step $\Delta t > 0$. In the following, $U_{h,0}^n$ will stand for a numerical approximation of $\tilde{U}_{h,0}(t^n)$, $U_{h,1}^n$ of $\tilde{U}_{h,1}(t^n)$ and Λ_h^n of $\tilde{\Lambda}_h(t^n)$ where $t^n = n\Delta t$. Moreover, $S_{h,i}^n$ is defined as $\tilde{S}_{h,i}(t^n)$.

The numerical discretization that we propose will be based on the following centered second order approximations of the second order time derivative of $\tilde{U}(t^n)$:

$$D_{\Delta t}^2 U_h^n := \frac{U_h^{n+1} - 2U_h^n + U_h^{n-1}}{\Delta t^2} \quad (11a)$$

and the centered second order “ θ -approximation” of $\tilde{U}(t^n)$:

$$\{U_h\}_\theta^n := \theta U_h^{n+1} + (1 - 2\theta)U_h^n + \theta U_h^{n-1} \quad (11b)$$

Let us state a simple result that comes from Taylor expansions of the previous quantities evaluated for a smooth function of time.

Proposition 1

Let $V(t) : \mathbb{R}^+ \rightarrow \mathbb{R}$ be a \mathcal{C}^{2p+2} function of time, with $p \in \mathbb{N}$ and $p \geq 2$. Then,

$$\begin{aligned} D_{\Delta t}^2 V^n &= \frac{d^2 V}{dt^2}(t^n) + \frac{\Delta t^2}{12} \frac{d^4 V}{dt^4}(t^n) + 2 \sum_{m=2}^p \frac{\Delta t^{2m}}{(2m+2)!} \frac{d^{2m+2} V}{dt^{2m+2}}(t^n) + \mathcal{O}(\Delta t^{2p+2}) \\ \{V\}_\theta^n &= V(t^n) + \theta \Delta t^2 \frac{d^2 V}{dt^2}(t^n) + 2\theta \Delta t^2 \sum_{m=1}^p \frac{\Delta t^{2m}}{(2m+2)!} \frac{d^{2m+2} V}{dt^{2m+2}}(t^n) + \mathcal{O}(\Delta t^{2p+2}) \end{aligned}$$

3.1. Implicit second order centered schemes: θ -schemes

The subset of conservative schemes among Newmark schemes (see chapter XX of [25]) constitutes the family of the so-called “ θ -schemes”. They read:

$$M_h D_{\Delta t}^2 U_h^n + K_h \{U_h\}_\theta^n = M_h S_h^n, \quad (12)$$

with $\theta \geq 0$ and where M_h stands for a positive symmetric definite mass matrix, K_h a positive symmetric semi-definite stiffness matrix and S_h^n for a source term. Notice that the specific choice $\theta = 0$ leads to an explicit scheme (the “leap-frog” scheme) while any other choice leads to an implicit scheme. Given a real parameter θ , the solution to (12) preserves the following discrete energy:

$$\mathcal{E}_{\theta,h}^{n+1/2} = \frac{1}{2} \left\| \frac{U_h^{n+1} - U_h^n}{\Delta t} \right\|_{\tilde{M}_h}^2 + \frac{1}{2} \left\| \frac{U_h^{n+1} + U_h^n}{2} \right\|_{K_h}^2 \quad (13)$$

where the modified mass matrix \tilde{M}_h is defined as

$$\tilde{M}_h = M_h + \Delta t^2 \left(\theta - \frac{1}{4} \right) K_h \quad (14)$$

The scheme (12) can be shown to be stable if the matrix \tilde{M}_h is positive. If $\theta \geq 1/4$, this is always true, hence the scheme is unconditionally stable. If $\theta < 1/4$, the scheme is stable provided that a stability condition is fulfilled. A consistency analysis shows that the scheme is second order accurate, unless $\theta = 1/12$ in which case fourth order of accuracy is achieved (this is called a “super-convergence” property).

3.2. Hybrid scheme

Let us consider a different implicit second order discretization on each part Ω_0 and Ω_1 of the domain Ω . Two implicit parameters θ_0 and θ_1 are introduced for respectively domain Ω_0 and domain Ω_1 . The coupling condition (7c) is first differentiated with respect to time, then discretized in a second order, centered way.

$$(\mathcal{P}_{01,h}^n) \begin{cases} M_{h,0} D_{\Delta t}^2 U_{h,0}^n + K_{h,0} \{U_{h,0}\}_{\theta_0}^n - {}^t C_{h,0} \Lambda_h^n = M_{h,0} S_{h,0}^n & (15a) \\ M_{h,1} D_{\Delta t}^2 U_{h,1}^n + K_{h,1} \{U_{h,1}\}_{\theta_1}^n + {}^t C_{h,1} \Lambda_h^n = M_{h,1} S_{h,1}^n & (15b) \\ C_{h,0} \frac{U_{h,0}^{n+1} - U_{h,0}^{n-1}}{2\Delta t} - C_{h,1} \frac{U_{h,1}^{n+1} - U_{h,1}^{n-1}}{2\Delta t} = 0 & (15c) \end{cases}$$

3.3. Algorithm

At each iteration the next iterates $(U_{h,0}^{n+1}, U_{h,1}^{n+1}, \Lambda_h^n)$ of system (15) are computed by solving a saddle point like system which matrix representation can be directly deduced from equations (15):

$$\begin{pmatrix} A_{h,0} & \mathbf{0} & -\Delta t^2 {}^t C_{h,0} \\ \mathbf{0} & A_{h,1} & \Delta t^2 {}^t C_{h,1} \\ -\Delta t^2 C_{h,0} & \Delta t^2 C_{h,1} & \mathbf{0} \end{pmatrix} \begin{pmatrix} U_{h,0}^{n+1} \\ U_{h,1}^{n+1} \\ \Lambda_h^n \end{pmatrix} = \begin{pmatrix} S_{h,0}^* \\ S_{h,1}^* \\ S_{h,\Gamma}^* \end{pmatrix} \quad (16)$$

with $A_{h,i} = M_{h,i} + \theta_i \Delta t^2 K_{h,i}$

$$S_{h,i}^* = M_{h,i} (\Delta t^2 S_{h,i}^n + 2U_{h,i}^n - U_{h,i}^{n-1}) - \Delta t^2 K_{h,i} ((1 - 2\theta_i)U_{h,i}^n + \theta_i U_{h,i}^{n-1})$$

$$S_{h,\Gamma}^* = -\Delta t^2 C_{h,0} U_{h,0}^{n-1} + \Delta t^2 C_{h,1} U_{h,1}^{n-1}$$

Since the matrices $A_{h,0}$ and $A_{h,1}$ are symmetric positive matrices, a sufficient condition for ensuring the invertibility of system (16) is the same as the semi-discrete case i.e. Eq. (10).

Direct Implicit-Explicit coupling Let us suppose that $\theta_0 = 0$. In this case, $A_{h,0}$ reduces to $M_{h,0}$. A Schur complement can be used to eliminate the volume unknowns of Ω_0 in system (16), then the following system must be inverted:

$$\begin{pmatrix} A_{h,1} & \Delta t^2 {}^t C_{h,1} \\ \Delta t^2 C_{h,1} & -\Delta t^4 C_{h,0} M_{h,0}^{-1} {}^t C_{h,0} \end{pmatrix} \begin{pmatrix} U_{h,1}^{n+1} \\ \Lambda_h^n \end{pmatrix} = \begin{pmatrix} S_{h,1}^* \\ S_{h,\Gamma}^* + \Delta t^2 C_{h,0} M_{h,0}^{-1} S_{h,0}^* \end{pmatrix} \quad (17)$$

After inverting this system, Λ_h^n is known and $U_{h,0}^{n+1}$ can be recovered by solving:

$$M_{h,0} U_{h,0}^{n+1} = S_{h,0}^* + \Delta t^2 {}^t C_{h,0} \Lambda_h^n \quad (18)$$

A simplification occurs when a mass lumping method is used to compute the mass matrix $M_{h,0}$ which is therefore diagonal. Such a method is compatible with standard \mathbb{P}_1 finite elements, high order spectral finite elements (see [2]) or mass lumping on augmented \mathbb{P}_2 finite element spaces (see [23] for triangular meshes or [24] for tetrahedral meshes). Another alternative is to use Interior Penalty Discontinuous Galerkin (IPDG) methods (see [19]) where the mass matrix is block-diagonal. In the situations mention above, the matrix $C_{h,0} M_{h,0}^{-1} {}^t C_{h,0}$ is a sparse interface matrix which does not induce a large overhead compared to the inversion of the matrix $A_{h,1}$ alone.

3.4. Energy preservation

The stability of scheme (15) relies on the following proposition:

Proposition 2

Any solution to (15) satisfies the energy identity:

$$\frac{\mathcal{E}_{01,h}^{n+1/2} - \mathcal{E}_{01,h}^{n-1/2}}{\Delta t} = M_{h,0} S_{h,0}^n \cdot \frac{U_{h,0}^{n+1} - U_{h,0}^{n-1}}{2\Delta t} + M_{h,1} S_{h,1}^n \cdot \frac{U_{h,1}^{n+1} - U_{h,1}^{n-1}}{2\Delta t} \quad (19)$$

where

$$\begin{aligned} \mathcal{E}_{01,h}^{n+1/2} = & \frac{1}{2} \left\| \frac{U_{h,0}^{n+1} - U_{h,0}^n}{\Delta t} \right\|_{\widetilde{M}_{h,0}}^2 + \frac{1}{2} \left\| \frac{U_{h,1}^{n+1} - U_{h,1}^n}{\Delta t} \right\|_{\widetilde{M}_{h,1}}^2 \\ & + \frac{1}{2} \left\| \frac{U_{h,0}^{n+1} + U_{h,0}^n}{2} \right\|_{K_{h,0}}^2 + \frac{1}{2} \left\| \frac{U_{h,1}^{n+1} + U_{h,1}^n}{2} \right\|_{K_{h,1}}^2 \end{aligned} \quad (20)$$

where the modified mass matrices are defined by

$$\widetilde{M}_{h,i} = M_{h,i} + \Delta t^2 \left(\theta_i - \frac{1}{4} \right) K_{h,i}, \text{ for } i \in \{0, 1\} \quad (21)$$

Proof

We multiply equation (15a) by $(U_{h,0}^{n+1} - U_{h,0}^{n-1})/2\Delta t$, equation (15b) by $(U_{h,1}^{n+1} - U_{h,1}^{n-1})/2\Delta t$ and equation (15c) by Λ_h^n . We then sum to get the expected result after noticing that the terms involving Λ_h^n cancel out. \square

The stability of the scheme will rely on the positivity of this energy, which is ensured by the following proposition.

Proposition 3

The discrete energy (20) is positive if the matrices $\widetilde{M}_{h,i}$ are positive for $i = \{0, 1\}$.

3.5. Stability

From the energy identity of proposition 2, it is possible to write an upper bound on the norm of the unknowns.

Proposition 4

Suppose that the energy (20) is positive. For any solution to (15) we have

$$\sqrt{\mathcal{E}_{01,h}^{n+1/2}} \leq \sqrt{\mathcal{E}_{01,h}^{1/2}} + \gamma(\theta_0, \theta_1) \frac{\Delta t}{\sqrt{2}} \sum_{\ell=1}^n \left[\|S_{h,0}^\ell\|_{M_{h,0}} + \|S_{h,1}^\ell\|_{M_{h,1}} \right] \quad (22)$$

where

$$\begin{aligned} \mathcal{E}_{01,h}^{1/2} = & \frac{1}{2} \left\| \frac{U_{h,0}^1 - U_{h,0}^0}{\Delta t} \right\|_{\widetilde{M}_{h,0}}^2 + \frac{1}{2} \left\| \frac{U_{h,1}^1 - U_{h,1}^0}{\Delta t} \right\|_{\widetilde{M}_{h,1}}^2 \\ & + \frac{1}{2} \left\| \frac{U_{h,0}^1 + U_{h,0}^0}{2} \right\|_{K_{h,0}}^2 + \frac{1}{2} \left\| \frac{U_{h,1}^1 + U_{h,1}^0}{2} \right\|_{K_{h,1}}^2 \end{aligned} \quad (23)$$

and $\gamma(\theta_0, \theta_1) = \max(\gamma(\theta_0), \gamma(\theta_1)) \leq 2\sqrt{2}$, where

$$\gamma(\theta) = \begin{cases} \frac{2}{a(\theta)} + \frac{2}{\sqrt{4 - (1 - 4\theta)a(\theta)^2}}, & \text{with } a(\theta) = \sqrt{\frac{4}{(1 - 4\theta)^{2/3} + (1 - 4\theta)}} \text{ if } \theta < 1/4 \\ 1 & \text{if } \theta \geq 1/4 \end{cases}$$

Then the solutions $U_{h,0}^{n+1}$ and $U_{h,1}^{n+1}$ can be bounded above as follows. For $i = \{0, 1\}$

$$\begin{aligned} \|U_{h,i}^{n+1}\|_{M_{h,i}} &\leq \|U_{h,i}^0\|_{M_{h,i}} + \sqrt{2}\gamma(\theta_i)t^{n+1}\sqrt{\mathcal{E}_{01,h}^{1/2}} \\ &\quad + \gamma(\theta_i)\gamma(\theta_0, \theta_1)\Delta t^2 \sum_{\ell=1}^n \sum_{k=1}^{\ell} \left[\|S_{h,0}^k\|_{M_{h,0}} + \|S_{h,1}^k\|_{M_{h,1}} \right] \end{aligned} \quad (24)$$

Proof

The reader can refer to [26] where a proof of this proposition is given when only one domain is involved. Two cases arise : $\theta_i \geq 1/4$ or $\theta_i < 1/4$. In the first case, it is easy to give an upper bound to the right hand side of equation (19) via the total energy since it is straightforward that for any vector X , $M_{h,i}X \cdot X \leq \widetilde{M}_{h,i}X \cdot X$. In the other case, a more involved proof is provided, which is still valid when the time step is chosen equal to its maximum allowed value (then $\widetilde{M}_{h,i}$ is singular hence the previous inequality does not hold for any vector X), based on a high frequency projector (see section 4.5 where this technique will be used). This proof is easily adapted to the present case. \square

Remark 3.1

Notice that the scheme (15), which couples two θ -schemes on domains Ω_0 and Ω_1 , is stable under the condition that each scheme is stable on its domain (from propositions 3 and 4). This is a satisfying condition since it does not lead to an additional constraint on the time step.

3.6. Consistency

We are now interested in the consistency of (15) with (7). To this purpose we define the errors terms:

$$e_{h,i}(t^n) = U_{h,i}^n - \widetilde{U}_{h,i}(t^n) \quad \text{and} \quad e_{h,\lambda}^n := \Lambda_h^n - \widetilde{\Lambda}_h(t^n)$$

Proposition 5

The error $(e_{h,0}, e_{h,1}, e_{h,\lambda})$ is solution to the system of equations:

$$\begin{cases} M_{h,0}D_{\Delta t}^2 e_{h,0}^n + K_{h,0}\{e_{h,0}\}_{\theta_0}^n - {}^tC_{h,0}e_{h,\lambda}^n = \Delta t^2 \widetilde{r}_{h,0}(t^n) + \mathcal{O}(\Delta t^4) & (25a) \\ M_{h,1}D_{\Delta t}^2 e_{h,1}^n + K_{h,1}\{e_{h,1}\}_{\theta_1}^n + {}^tC_{h,1}e_{h,\lambda}^n = \Delta t^2 \widetilde{r}_{h,1}(t^n) + \mathcal{O}(\Delta t^4) & (25b) \\ C_{h,0}\frac{e_{h,0}^{n+1} - e_{h,0}^{n-1}}{2\Delta t} - C_{h,1}\frac{e_{h,1}^{n+1} - e_{h,1}^{n-1}}{2\Delta t} = 0 & (25c) \end{cases}$$

where

$$\begin{cases} \widetilde{r}_{h,0}(t^n) = \left(\theta_0 - \frac{1}{12}\right) \left(K_{h,0}M_{h,0}^{-1} \left[K_{h,0}\widetilde{U}_{h,0}(t^n) - {}^tC_{h,0}\widetilde{\Lambda}_h(t^n) \right] - K_{h,0}\widetilde{S}_{h,0}(t^n) \right) \\ \quad - \frac{1}{12} {}^tC_{h,0} \frac{d^2}{dt^2} \widetilde{\Lambda}_h(t^n) - \frac{1}{12} M_{h,0} \frac{d^2}{dt^2} \widetilde{S}_{h,0}(t^n) \\ \widetilde{r}_{h,1}(t^n) = \left(\theta_1 - \frac{1}{12}\right) \left(K_{h,1}M_{h,1}^{-1} \left[K_{h,1}\widetilde{U}_{h,1}(t^n) + {}^tC_{h,1}\widetilde{\Lambda}_h(t^n) \right] - K_{h,1}\widetilde{S}_{h,1}(t^n) \right) \\ \quad + \frac{1}{12} {}^tC_{h,1} \frac{d^2}{dt^2} \widetilde{\Lambda}_h(t^n) - \frac{1}{12} M_{h,1} \frac{d^2}{dt^2} \widetilde{S}_{h,1}(t^n) \end{cases} \quad (26)$$

This system of equations on the error shows that the scheme (15) is consistent with the semi discrete system (7) up to order two since the error satisfies equation (7) where the source terms are of the order of $\mathcal{O}(\Delta t^2)$.

Proof

We compute the quantity

$$\begin{aligned} M_{h,0} D_{\Delta t}^2 e_{h,0}^n + K_{h,0} \{e_{h,0}\}_{\theta_0}^n = \\ \underbrace{M_{h,0} D_{\Delta t}^2 U_{h,0}^n + K_{h,0} \{U_{h,0}\}_{\theta_0}^n}_{= {}^t C_{h,0} \Lambda_h^n + M_{h,0} S_{h,0}^n \text{ because of (15)}} - \left(M_{h,0} D_{\Delta t}^2 \tilde{U}_{h,0} + K_{h,0} \{\tilde{U}_{h,0}\}_{\theta_0}^n \right) \end{aligned} \quad (27)$$

Let us use proposition 1 in order to replace the last two terms by their Taylor expansion, and use the fact that $\tilde{U}_{h,0}(t)$ is solution to (7) in order to simplify the terms of order zero in Δt , we obtain

$$\begin{aligned} M_{h,0} D_{\Delta t}^2 \tilde{U}_{h,0} + K_{h,0} \{\tilde{U}_{h,0}\}_{\theta_0}^n = {}^t C_{h,0} \tilde{\Lambda}_h(t^n) + M_{h,0} \tilde{S}_{h,0}(t^n) \\ + \Delta t^2 \left[\frac{1}{12} M_{h,0} \frac{d^4 \tilde{U}_{h,0}}{dt^4}(t^n) + \theta_0 K_{h,0} \frac{d^2 \tilde{U}_{h,0}}{dt^2}(t^n) \right] + \mathcal{O}(\Delta t^4) \end{aligned} \quad (28)$$

At this point we have to use again the semi discrete equation (7), this gives

$$\begin{cases} K_{h,0} \frac{d^2 \tilde{U}_{h,0}}{dt^2}(t^n) = -K_{h,0} M_{h,0}^{-1} K_{h,0} \tilde{U}_{h,0}(t^n) + K_{h,0} M_{h,0}^{-1} {}^t C_{h,0} \tilde{\Lambda}_h(t^n) + K_{h,0} \tilde{S}_{h,0}(t^n) \\ M_{h,0} \frac{d^4 \tilde{U}_{h,0}}{dt^4}(t^n) = -K_{h,0} \frac{d^2 \tilde{U}_{h,0}}{dt^2}(t^n) + {}^t C_{h,0} \frac{d^2 \tilde{\Lambda}_h}{dt^2}(t^n) + M_{h,0} \frac{d^2 \tilde{S}_{h,0}}{dt^2}(t^n) \end{cases}$$

Therefore, (28) becomes

$$M_{h,0} D_{\Delta t}^2 \tilde{U}_{h,0} + K_{h,0} \{\tilde{U}_{h,0}\}_{\theta_0}^n = {}^t C_{h,0} \tilde{\Lambda}_h(t^n) + M_{h,0} \tilde{S}_{h,0}(t^n) - \Delta t^2 \tilde{r}_{h,0}(t^n) + \mathcal{O}(\Delta t^4)$$

where $\tilde{r}_{h,0}(t^n)$ is defined as (26). Recall that $S_{h,i}^n = \tilde{S}_{h,i}(t^n)$. Hence by combining the previous equation with (27) we get (25a). Same arguments apply to the other domain to get (25b). The last equation (26) is straightforward using (7c). \square

Remark 3.2

Notice that if $\theta_0 = \theta_1 = 1/12$, we expect to have a fourth order approximation in time $U_{h,0}^n$ of $\tilde{U}_{h,0}(t^n)$, $U_{h,1}^n$ of $\tilde{U}_{h,1}(t^n)$, even if Λ_h^n will only be a second order approximation of $\tilde{\Lambda}_h(t^n)$. This can be understood (assume for simplicity that the source terms vanish) by writing system (25) as follows:

$$\begin{cases} M_{h,0} D_{\Delta t}^2 e_{h,0}^n + K_{h,0} \{e_{h,0}\}_{1/12}^n = {}^t C_{h,0} \left[e_{h,\lambda}^n - \frac{\Delta t^2}{12} \frac{d^2}{dt^2} \tilde{\Lambda}_h(t^n) \right] + \mathcal{O}(\Delta t^4) \\ M_{h,1} D_{\Delta t}^2 e_{h,1}^n + K_{h,1} \{e_{h,1}\}_{1/12}^n = -{}^t C_{h,1} \left[e_{h,\lambda}^n + \frac{\Delta t^2}{12} \frac{d^2}{dt^2} \tilde{\Lambda}_h(t^n) \right] + \mathcal{O}(\Delta t^4) \\ C_{h,0} \frac{e_{h,0}^{n+1} - e_{h,0}^{n-1}}{2\Delta t} - C_{h,1} \frac{e_{h,1}^{n+1} - e_{h,1}^{n-1}}{2\Delta t} = 0 \end{cases}$$

which can be seen as system (15) with a modified Lagrange multiplier.

Remark 3.3 (Splitting)

A valid alternative in the case of conformal meshes is to split algebraically the equation

$$M_h d_t^2 \tilde{U}_h + K_h \tilde{U}_h = 0 \quad (30)$$

into the following one, with $M = M_{h,0} + M_{h,1}$, and $K = K_{h,0} + K_{h,1}$,

$$M_{h,0} d_t^2 \tilde{U}_h + M_{h,1} d_t^2 \tilde{U}_h + K_{h,0} \tilde{U}_h + K_{h,1} \tilde{U}_h = 0 \quad (31)$$

It is then possible to consider the following hybrid scheme :

$$M_{h,0} D_{\Delta t}^2 U_h^n + M_{h,1} D_{\Delta t}^2 U_h^n + K_{h,0} \{U_h\}_{\theta_0}^n + K_{h,1} \{U_h\}_{\theta_1}^n = 0 \quad (32)$$

which can lead to several discretizations depending on the way the matrices are split. This approach can be linked to Implicit-Explicit (IMEX) schemes [16]. This scheme preserves the following energy

$$\mathcal{E}_h^{n+1/2} = \widetilde{M}_h \frac{U_h^{n+1} - U_h^n}{\Delta t} \cdot \frac{U_h^{n+1} - U_h^n}{\Delta t} + K_h \frac{U_h^{n+1} + U_h^n}{2} \cdot \frac{U_h^{n+1} + U_h^n}{2} \quad (33)$$

where

$$\widetilde{M}_h = M_{h,0} + M_{h,1} + \Delta t^2(\theta_0 - \frac{1}{4})K_{h,0} + \Delta t^2(\theta_1 - \frac{1}{4})K_{h,1} \quad (34)$$

This scheme is therefore stable as soon as each θ_i -scheme is stable for the sub-problem associated to the matrices $(M_{h,i}, K_{h,i})$ for $i \in \{1, 2\}$. Notice however that the resulting scheme is not equivalent to scheme (15) since the unknowns U_h are not separated into two groups: here an overlapping zone exists. We did not choose to generalize this approach to fourth order because the stability properties of the resulting modified scheme were less promising (see remark 4.5).

3.7. Numerical illustration

In this section we present numerical illustrations obtained with scheme (15) in 1D along with high order spectral finite elements using the mass lumping method. We consider the 1D scalar wave equation with velocity equal to 1 m/s in a domain of length 1 m with periodic boundary conditions:

$$\partial_t^2 u(x, t) - \partial_x^2 u(x, t) = 0, \quad x \in [0, 1], \quad u(0, t) = u(1, t), \quad \partial_x u(0, t) = \partial_x u(1, t). \quad (35)$$

The initial condition is a pulse centered around $x_0 = 0.2$. The initial velocity is such that the analytic solution is this pulse traveling from left to right. More precisely, the initial condition reads:

$$u(x, 0) = u_0(x) = \begin{cases} e^{-\frac{1}{1-100(x-x_0)^2}} & \text{if } |x - x_0| < 0.1 \\ 0 & \text{otherwise} \end{cases} \quad (36)$$

The analytic solution is given by

$$u(x, t) = u_0(x - t + n) \quad \text{where } n \in \mathbb{N} \text{ such that } x - t + n \in [0, 1]. \quad (37)$$

In order to represent the kind of difficulties that we aim at tackling in this work, the interval $[0, 1]$ is artificially divided in two parts: $[0, 0.5]$ where the mesh is coarse and $[0.5, 1]$ where the mesh is fine. In a first illustrative experiment, we use 7 elements on $[0, 0.5]$ and 13 elements on $[0.5, 1]$. Then spectral finite elements of order 6 are used. This choice ensures that the spatial discretization is fine enough to be able to impute to time discretization the error between the numerical and analytical solutions. The final time of the simulation is 0.5 sec. If an explicit scheme was used everywhere in the domain, the time step restriction would be

$$\Delta t \leq 2.8 \times 10^{-3} \text{ sec.} \quad (38)$$

Using an explicit scheme on the left-hand side of the domain and a 1/4-scheme on the right hand side, the time step restriction becomes

$$\Delta t \leq 5.2 \times 10^{-3} \text{ sec.} \quad (39)$$

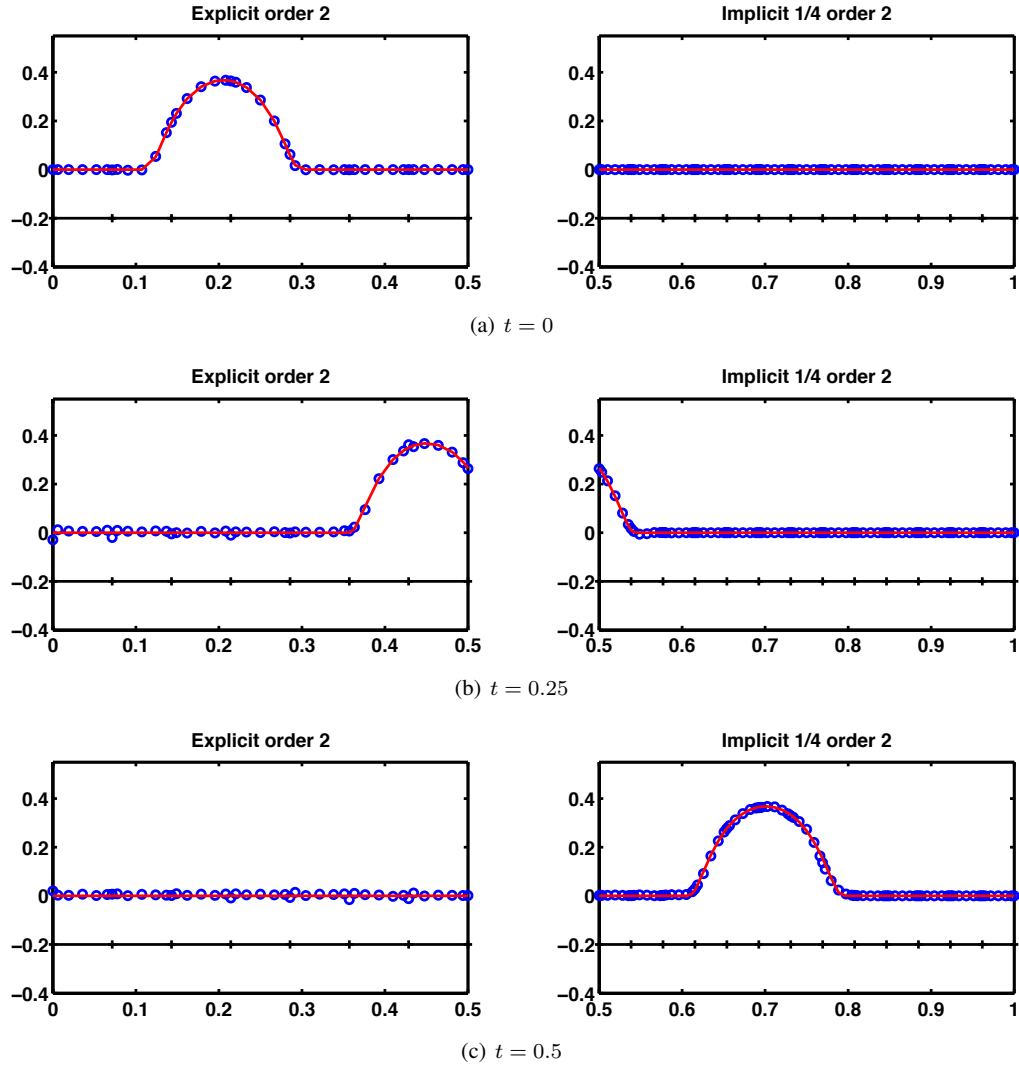


Figure 1. Snapshots of the analytical solution (in red solid line) and numerical solution (in blue circles). In black is displayed the mesh on each part of the domain.

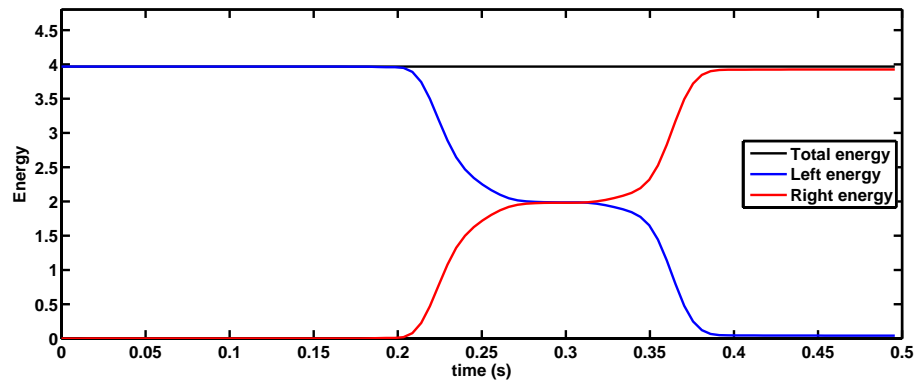
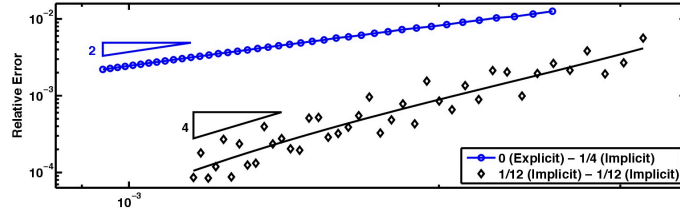


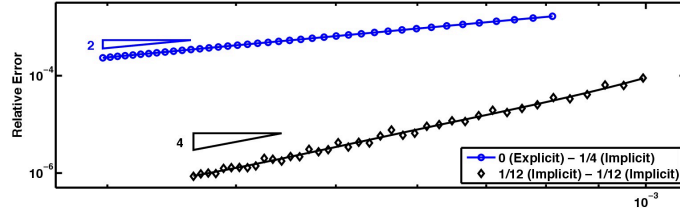
Figure 2. Total energy evolution

We chose Δt such that (39) is an equality. In Fig. 1 are displayed snapshots of the solution at times $t = 0$, $t = 0.25$ and $t = 0.5$ sec in blue circles, along with the analytical solution in solid red line. The pulse travels from one domain to the other as expected. The maximal value of the relative L2 error with the analytical solution along time is 6.24×10^{-2} . Numerical dispersion is visible and is due to the lack of precision of the time discretization. The discrete energy of the numerical solution is computed for each time step following formula (20). The relative total energy deviation is comparable to machine precision (10^{-14}). The total energy is plotted in Fig. 2 along with the energies of each sub-domain.

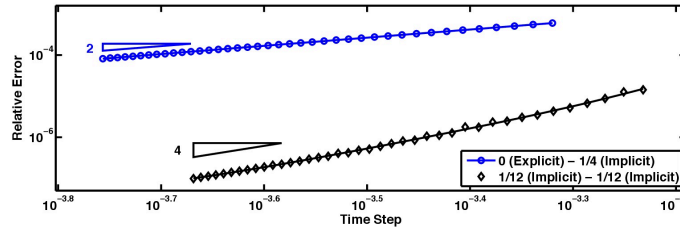
In figure 3 are displayed spatio-temporal convergence curves that arise from similar numerical experiments using third, sixth and eighth order finite elements in space. The mesh size h tends to zero for obtaining these curves, and the time step Δt is chosen as the largest Δt such that the matrices $\widetilde{M}_{h,1}$ and $\widetilde{M}_{h,2}$ defined in Eq. (21) are positive. The previous coupled scheme (explicit / 1/4-scheme) is performed with a mesh having $5 + 2N$, $N \in [20, 60]$ uniform elements in the explicit region, and $8 + 4N$ elements in the implicit region. It leads to the curves with blue circles which show a second order convergence rate as expected. Another series of curves have been obtained by coupling two 1/12-schemes together, with the same number of elements on each subinterval, equal to $5 + 2N$, with the second order coupling condition proposed in system (15). The convergence rate appears to be in average of order four, illustrating remark 3.2.



(a) Third Order Finite Elements



(b) Sixth Order Finite Elements



(c) Eighth Order Finite Elements

Figure 3. Maximal relative L2 error with the analytic solution along time for scheme (15).

4. FOURTH ORDER CONSERVATIVE HYBRID SCHEMES

We have developed in [15] new fourth order accurate implicit schemes, using the modified equation method. Let us begin this section with a short introduction to these numerical schemes.

4.1. Short presentation of the (θ, φ) -schemes

This family of schemes depend on two parameters θ and φ , which are real numbers to be determined. These schemes read:

$$M_h D_{\Delta t}^2 U_h + K_h \{U_h\}_\theta^n + \Delta t^2 \left(\theta - \frac{1}{12} \right) K_h M_h^{-1} K_h \{U_h\}_\varphi^n = M_h S_h^n \quad (40)$$

Assuming that the source term is regular enough the global fourth order consistency is preserved by defining a modified source term S_h^n as (see remark 4.2 of [15]):

$$S_h^n = \tilde{S}_h(t^n) + \frac{\Delta t^2}{12} \frac{d^2 \tilde{S}_h}{dt^2}(t^n) + \Delta t^2 \left(\theta - \frac{1}{12} \right) M_h^{-1} K_h \tilde{S}_h(t^n). \quad (41)$$

Given a pair (θ, φ) , the solution to (40) satisfies the following energy identity:

$$\frac{\mathcal{E}_{(\theta, \varphi), h}^{n+1/2} - \mathcal{E}_{(\theta, \varphi), h}^{n-1/2}}{\Delta t} = M_h S_h^n \cdot \frac{U_h^{n+1} - U_h^{n-1}}{2\Delta t} \quad (42)$$

where the discrete energy is defined as:

$$\mathcal{E}_{(\theta, \varphi), h}^{n+1/2} = \frac{1}{2} \left\| \frac{U_h^{n+1} - U_h^n}{\Delta t} \right\|_{\tilde{M}_h}^2 + \frac{1}{2} \left\| \frac{U_h^{n+1} + U_h^n}{2} \right\|_{\tilde{K}_h}^2 \quad (43)$$

This expression involves modified mass and stiffness matrices defined as:

$$\tilde{M}_h = M_h + \Delta t^2 \left(\theta - \frac{1}{4} \right) K_h + \Delta t^4 \left(\theta - \frac{1}{12} \right) \left(\varphi - \frac{1}{4} \right) K_h M_h^{-1} K_h \quad (44)$$

$$\tilde{K}_h = K_h + \Delta t^2 \left(\theta - \frac{1}{12} \right) K_h M_h^{-1} K_h \quad (45)$$

The scheme (40) can be shown to be stable and at least fourth order accurate if the matrices \tilde{M}_h and \tilde{K}_h are positive. As it is not always satisfied, this requirement leads to a CFL-like condition i.e. an upper bound on the time step, which depends on the pair (θ, φ) . Notice that the $(1/4, 1/4)$ -scheme is for example unconditionally stable. Other values of (θ, φ) give remarkable schemes studied in [15] obtained after optimization regarding the consistency or regarding the computational cost.

Remark 4.1

We introduce the matrix \tilde{I}_h as

$$\tilde{I}_h = I_h + \Delta t^2 \left(\theta - \frac{1}{12} \right) K_h M_h^{-1} \quad (46)$$

where I_h stands for the identity matrix in the appropriate finite dimensional space. Multiplying Eq. (40) by \tilde{I}_h^{-1} one can show another energy identity, which reads :

$$\frac{\tilde{\mathcal{E}}_{(\theta, \varphi), h}^{n+1/2} - \tilde{\mathcal{E}}_{(\theta, \varphi), h}^{n-1/2}}{\Delta t} = \tilde{I}_h^{-1} M_h S_h^n \cdot \frac{U_h^{n+1} - U_h^{n-1}}{2\Delta t} \quad (47)$$

where another discrete energy is defined:

$$\tilde{\mathcal{E}}_{(\theta,\varphi),h}^{n+1/2} = \frac{1}{2} \left\| \frac{U_h^{n+1} - U_h^n}{\Delta t} \right\|_{\widehat{M}_h}^2 + \frac{1}{2} \left\| \frac{U_h^{n+1} + U_h^n}{2} \right\|_{K_h}^2 \quad (48)$$

for which only a symmetric modified mass matrix has to be introduced:

$$\widehat{M}_h = \widetilde{I}_h^{-1} \widetilde{M}_h, \quad \widetilde{I}_h \text{ defined in (46) and } \widetilde{M}_h \text{ in (44)} \quad (49)$$

We will see that this unusual energy will be the one appearing in the fourth order hybrid scheme presented below. Note that the symmetry of \widehat{M}_h is a consequence of the symmetry of

$$M_h^{-1/2} \widehat{M}_h M_h^{-1/2} = \left(M_h^{-1/2} \widetilde{I}_h M_h^{1/2} \right)^{-1} \left(M_h^{-1/2} \widetilde{M}_h M_h^{-1/2} \right).$$

Note that both terms of this product are polynomials of the symmetric matrix $M_h^{-1/2} K_h M_h^{-1/2}$ hence have an eigen-decomposition in the same basis, which ensures the symmetry.

4.2. Hybrid schemes

Ensuring an appropriate coupling of such schemes is not straightforward because of a possible loss of accuracy. Naive coupling conditions are indeed not adapted to the modified equation procedure as it will be illustrated in the numerical results section, especially Figure 6.

We propose to study the following scheme, which is motivated by the consistency analysis of section 3.6. A new denomination of the Lagrange multiplier is used: Π_h^n , this change of notation is motivated by the consistency analysis given in section 4.6.

$$\begin{cases} M_{h,0} D_{\Delta t}^2 U_{h,0}^n + K_{h,0} \{U_{h,0}\}_{\theta_0}^n - {}^t C_{h,0} \Pi_h^n = \\ M_{h,0} S_{h,0}^n + \Delta t^2 \left(\theta_0 - \frac{1}{12} \right) K_{h,0} M_{h,0}^{-1} [-K_{h,0} \{U_{h,0}\}_{\varphi_0}^n + {}^t C_{h,0} \Pi_h^n] \end{cases} \quad (50a)$$

$$\begin{cases} M_{h,1} D_{\Delta t}^2 U_{h,1}^n + K_{h,1} \{U_{h,1}\}_{\theta_1}^n + {}^t C_{h,1} \Pi_h^n = \\ M_{h,1} S_{h,1}^n + \Delta t^2 \left(\theta_1 - \frac{1}{12} \right) K_{h,1} M_{h,1}^{-1} [-K_{h,1} \{U_{h,1}\}_{\varphi_1}^n - {}^t C_{h,1} \Pi_h^n] \end{cases} \quad (50b)$$

$$C_{h,0} \frac{U_{h,0}^{n+1} - U_{h,0}^{n-1}}{2\Delta t} - C_{h,1} \frac{U_{h,1}^{n+1} - U_{h,1}^{n-1}}{2\Delta t} = 0 \quad (50c)$$

4.3. Algorithm

Before studying the properties, we present a possible method for solving system (50). In a first step we present a method for any implicit-implicit coupling, then in a second step we present the modifications that occur when one of the domains is treated explicitly.

4.3.1. Direct inversion of the system Assuming that φ_0 and φ_1 are non zero, we must solve on each subdomain (see [15] for more details)

$$A_{h,i} \{U_{h,i}\}_{\varphi_i}^n = S_{h,i}^* + \varphi_i \Delta t^2 (-1)^i \widetilde{I}_{h,i} {}^t C_{h,i} \Pi_h^n \quad (51)$$

where

$$\begin{cases} A_{h,i} = M_{h,i} + \Delta t^2 \theta_i K_{h,i} + \Delta t^4 \varphi_i \left(\theta_i - \frac{1}{12} \right) K_{h,i} M_{h,i}^{-1} K_{h,i} \\ \widetilde{I}_{h,i} = I_h + \Delta t^2 \left(\theta_i - \frac{1}{12} \right) K_{h,i} M_{h,i}^{-1} \\ S_{h,i}^* = \Delta t^2 \varphi_i M_{h,i} S_{h,i}^n + [M_{h,i} - \Delta t^2 (\varphi_i - \theta_i) K_{h,i}] U_{h,i}^n \end{cases} \quad (52)$$

and equation (50c) written for the unknowns $\{U_{h,i}\}_{\varphi_i}^n$ gives:

$$-C_{h,0} \left[\frac{\Delta t^2}{\varphi_0} \{U_{h,0}\}_{\varphi_0}^n - \frac{\Delta t^2}{\varphi_0} (1 - 2\varphi_0) U_{h,0}^n - 2\Delta t^2 U_{h,0}^{n-1} \right] + \\ C_{h,1} \left[\frac{\Delta t^2}{\varphi_1} \{U_{h,1}\}_{\varphi_1}^n - \frac{\Delta t^2}{\varphi_1} (1 - 2\varphi_1) U_{h,1}^n - 2\Delta t^2 U_{h,1}^{n-1} \right] = 0 \quad (53)$$

The existence of a discrete solution to (50) is ensured by the invertibility of the matrix

$$\begin{pmatrix} \frac{1}{\varphi_0^2} \tilde{I}_{h,0}^{-1} A_{h,0} & \mathbf{0} & -\frac{\Delta t^2}{\varphi_0} {}^t C_{h,0} \\ \mathbf{0} & \frac{1}{\varphi_1^2} \tilde{I}_{h,1}^{-1} A_{h,1} & \frac{\Delta t^2}{\varphi_1} {}^t C_{h,1} \\ -\frac{\Delta t^2}{\varphi_0} C_{h,0} & \frac{\Delta t^2}{\varphi_1} C_{h,1} & \mathbf{0} \end{pmatrix}$$

Assuming that the symmetric matrix $\tilde{I}_{h,i}^{-1} A_{h,i}$ is positive, Eq. (10) is a sufficient condition. However, inverting directly this matrix is not convenient because it includes matrices products and it has a wider bandwidth. To avoid this difficulty, by algebraic manipulations of equations (52) one can decompose $A_{h,i}$ as follows

$$A_{h,i} = \tilde{I}_{h,i} \left[M_{h,i} + \frac{\Delta t^2}{12} K_{h,i} \right] + \Delta t^4 \left(\varphi_i - \frac{1}{12} \right) \left(\theta_i - \frac{1}{12} \right) K_{h,i} M_{h,i}^{-1} K_{h,i} \quad (54)$$

Then, assuming that $(\varphi_i - \frac{1}{12})(\theta_i - \frac{1}{12}) > 0$ it is useful to introduce the unknown $V_{h,i}^n$ such that (recall that the matrix $\tilde{I}_{h,i}$ commutes with $K_{h,i} M_{h,i}^{-1}$ since it is a polynomial of $K_{h,i} M_{h,i}^{-1}$)

$$\tilde{I}_{h,i} M_{h,i} V_{h,i}^n - \Delta t^2 \sqrt{\alpha_i} K_{h,i} \{U_{h,i}\}_{\varphi_i}^n = 0, \quad \text{where } \alpha_i = (\varphi_i - \frac{1}{12})(\theta_i - \frac{1}{12}) \quad (55)$$

Equation (51) then becomes

$$\left[M_{h,i} + \frac{\Delta t^2}{12} K_{h,i} \right] \{U_{h,i}\}_{\varphi_i}^n + \Delta t^2 \sqrt{\alpha_i} K_{h,i} V_{h,i}^n = (-1)^i \Delta t^2 \varphi_i {}^t C_{h,i} \Pi_h^n + \tilde{I}_{h,i}^{-1} S_{h,i}^*$$

This gives the following augmented system:

$$R_h \begin{pmatrix} \{U_{h,0}\}_{\varphi_0}^n \\ V_{h,0} \\ \{U_{h,1}\}_{\varphi_1}^n \\ V_{h,1} \\ \Pi_h^n \end{pmatrix} = \begin{pmatrix} \frac{1}{\varphi_0^2} \tilde{I}_{h,0}^{-1} S_{h,0}^* \\ 0 \\ \frac{1}{\varphi_1^2} \tilde{I}_{h,1}^{-1} S_{h,1}^* \\ 0 \\ S_{h,\Gamma}^* \end{pmatrix} \quad (56)$$

where $R_h = A_h + \Delta t^2 B_h$, with A_h symmetric and B_h skew-symmetric:

$$A_h = \begin{pmatrix} \frac{1}{\varphi_0^2} \left[M_{h,0} + \frac{\Delta t^2}{12} K_{h,0} \right] & 0 & 0 & 0 & -\frac{\Delta t^2}{\varphi_0} {}^t C_{h,0} \\ 0 & \frac{1}{\varphi_0^2} \tilde{I}_{h,0} M_{h,0} & 0 & 0 & 0 \\ 0 & 0 & \frac{1}{\varphi_1^2} \left[M_{h,1} + \frac{\Delta t^2}{12} K_{h,1} \right] & 0 & \frac{\Delta t^2}{\varphi_1} {}^t C_{h,1} \\ 0 & 0 & 0 & \frac{1}{\varphi_1^2} \tilde{I}_{h,1} M_{h,1} & 0 \\ -\frac{\Delta t^2}{\varphi_0} C_{h,0} & 0 & \frac{\Delta t^2}{\varphi_1} C_{h,1} & 0 & 0 \end{pmatrix}$$

$$B_h = \begin{pmatrix} 0 & \frac{\sqrt{\alpha_0}}{\varphi_0^2} K_{h,0} & 0 & 0 & 0 \\ -\frac{\sqrt{\alpha_0}}{\varphi_0^2} K_{h,0} & 0 & 0 & 0 & 0 \\ 0 & 0 & 0 & \frac{\sqrt{\alpha_1}}{\varphi_1^2} K_{h,1} & 0 \\ 0 & 0 & -\frac{\sqrt{\alpha_1}}{\varphi_1^2} K_{h,1} & 0 & 0 \\ 0 & 0 & 0 & 0 & 0 \end{pmatrix}$$

$$S_{h,\Gamma}^* = \Delta t^2 C_{h,1} \left[\frac{1-2\varphi_1}{\varphi_1} U_{h,1}^n + 2U_{h,1}^{n-1} \right] - \Delta t^2 C_{h,0} \left[\frac{1-2\varphi_0}{\varphi_0} U_{h,0}^n + 2U_{h,0}^{n-1} \right]$$

4.3.2. Direct inversion of the Implicit-Explicit coupling system Let us consider the case where $(\theta_0, \varphi_0) = (0, 0)$. As in the previous section, some simplifications are possible. In this case, the system to solve reads:

$$\begin{pmatrix} M_{h,0} & \mathbf{0} & -\Delta t^2 \tilde{I}_{h,0} {}^t C_{h,0} \\ \mathbf{0} & \frac{1}{\varphi_1^2} \tilde{I}_{h,1}^{-1} A_{h,1} & \frac{\Delta t^2}{\varphi_1} {}^t C_{h,1} \\ -\Delta t^2 C_{h,0} & \frac{\Delta t^2}{\varphi_1} C_{h,1} & \mathbf{0} \end{pmatrix} \begin{pmatrix} U_{h,0}^{n+1} \\ \{U_{h,1}^{n+1}\}_{\varphi_1}^n \\ \Pi_h^n \end{pmatrix} = \begin{pmatrix} S_{h,0}^{**} \\ S_{h,1}^* \\ S_{h,\Gamma}^{**} \end{pmatrix} \quad (57)$$

where

$$\begin{aligned} S_{h,0}^{**} &= -\Delta t^2 \tilde{I}_{h,0} K_{h,0} U_{h,0}^n + \Delta t^2 M_{h,0} S_{h,0}^n + 2M_{h,0} U_{h,0}^n - M_{h,0} U_{h,0}^{n-1} \\ S_{h,\Gamma}^{**} &= \Delta t^2 C_{h,1} \left[\frac{1-2\varphi_1}{\varphi_1} U_{h,1}^n + 2U_{h,1}^{n-1} \right] + \Delta t^2 C_{h,0} U_{h,0}^{n-1} \end{aligned}$$

A Schur complement of (57) allows to eliminate the unknowns $U_{h,0}$:

$$\begin{pmatrix} \frac{1}{\varphi_1^2} \tilde{I}_{h,1}^{-1} A_{h,1} & \frac{\Delta t^2}{\varphi_1} {}^t C_{h,1} \\ \frac{\Delta t^2}{\varphi_1} C_{h,1} & -\Delta t^4 C_{h,0} M_{h,0}^{-1} \tilde{I}_{h,0} {}^t C_{h,0} \end{pmatrix} \begin{pmatrix} \{U_{h,1}^{n+1}\}_{\varphi_1}^n \\ \Pi_h^n \end{pmatrix} = \begin{pmatrix} S_{h,1}^* \\ S_{h,\Gamma}^{**} + \Delta t^2 C_{h,0} M_{h,0}^{-1} S_{h,0}^{**} \end{pmatrix} \quad (58)$$

Once again, this system requires the inversion of matrix polynomials due to the presence of $A_{h,1}$. Our algorithmic strategy is to introduce the intermediary unknown $V_{h,1}$ as previously described (see Eq. (55)). Moreover, using the mass lumping method, the matrix $C_{h,0} M_{h,0}^{-1} \tilde{I}_{h,0} {}^t C_{h,0}$ is a sparse interface matrix therefore solving (58) does not induce a large over-cost compared to the inversion of the matrix $\tilde{I}_{h,1}^{-1} A_{h,1}$ alone.

4.4. Energy preservation

The stability of scheme (50) relies on the following proposition.

Proposition 6

Any solution to (50) satisfies the energy identity:

$$\frac{\mathcal{E}_{01,4,h}^{n+1/2} - \mathcal{E}_{01,4,h}^{n-1/2}}{\Delta t} = \tilde{I}_{h,0}^{-1} M_{h,0} S_{h,0}^n \cdot \frac{U_{h,0}^{n+1} - U_{h,0}^{n-1}}{2\Delta t} + \tilde{I}_{h,1}^{-1} M_{h,1} S_{h,1}^n \cdot \frac{U_{h,1}^{n+1} - U_{h,1}^{n-1}}{2\Delta t}, \quad (59)$$

where

$$\begin{aligned} \mathcal{E}_{01,4,h}^{n+1/2} &= \frac{1}{2} \left\| \frac{U_{h,0}^{n+1} - U_{h,0}^n}{\Delta t} \right\|_{\widehat{M}_{h,0}}^2 + \frac{1}{2} \left\| \frac{U_{h,1}^{n+1} - U_{h,1}^n}{\Delta t} \right\|_{\widehat{M}_{h,1}}^2 \\ &\quad + \frac{1}{2} \left\| \frac{U_{h,0}^{n+1} + U_{h,0}^n}{2} \right\|_{K_{h,0}}^2 + \frac{1}{2} \left\| \frac{U_{h,1}^{n+1} + U_{h,1}^n}{2} \right\|_{K_{h,1}}^2 \end{aligned} \quad (60)$$

and where the modified mass matrices $\widehat{M}_{h,i}$ are defined by:

$$\widehat{M}_{h,i} = \tilde{I}_{h,i}^{-1} \widetilde{M}_{h,i} \quad (61)$$

with

$$\left\{ \begin{aligned} \widetilde{I}_{h,i} &= I_{h,i} + \Delta t^2 \left(\theta_i - \frac{1}{12} \right) K_{h,i} M_{h,i}^{-1} \end{aligned} \right. \quad (62a)$$

$$\left\{ \begin{aligned} \widetilde{M}_{h,i} &= M_{h,i} + \Delta t^2 \left(\theta_i - \frac{1}{4} \right) K_{h,i} + \Delta t^4 \left(\theta_i - \frac{1}{12} \right) \left(\varphi_i - \frac{1}{4} \right) K_{h,i} M_{h,i}^{-1} K_{h,i} \end{aligned} \right. \quad (62b)$$

Proof

We first re-write (50a) and (50b) as follows

$$\widetilde{M}_{h,i} D_{\Delta t}^2 U_{h,i}^n + \widetilde{K}_{h,i} \{U_{h,i}^n\}_{1/4}^n - (-1)^i \widetilde{I}_{h,i} {}^t C_{h,i} \Pi_h^n = M_{h,i} S_{h,i}^n \quad (63)$$

where the modified matrices are the matrices appearing in the (θ, φ) -scheme

$$\begin{cases} \widetilde{K}_{h,i} = K_{h,i} + \Delta t^2 \left(\theta_i - \frac{1}{12} \right) K_{h,i} M_{h,i}^{-1} K_{h,i} \\ \widetilde{M}_{h,i} \text{ defined as (62b) and } \widetilde{I}_{h,i} \text{ defined as (62a)} \end{cases} \quad (64a)$$

$$\quad (64b)$$

The naive idea (coming from the previous analysis) would be to multiply the obtained equation (63) by $(U_{h,i}^{n+1} - U_{h,i}^{n-1})/2\Delta t$ and then sum over i . We get:

$$\frac{\mathcal{E}_{(\theta,\varphi),h}^{n+1/2}(U_{h,0}) + \mathcal{E}_{(\theta,\varphi),h}^{n+1/2}(U_{h,1}) - \mathcal{E}_{(\theta,\varphi),h}^{n-1/2}(U_{h,0}) - \mathcal{E}_{(\theta,\varphi),h}^{n-1/2}(U_{h,1})}{\Delta t} = \Pi_h^n \cdot \left[C_{h,0} \widetilde{I}_{h,0} \frac{U_{h,0}^{n+1} - U_{h,0}^{n-1}}{2\Delta t} - C_{h,1} \widetilde{I}_{h,1} \frac{U_{h,1}^{n+1} - U_{h,1}^{n-1}}{2\Delta t} \right] \quad (65)$$

where the energy $\mathcal{E}_{(\theta,\varphi),h}^{n+1/2}(U_{h,i})$ is defined as the (θ, φ) -scheme energy on the domain Ω_i (see (43)). The reader can see that the term inside the brackets is not the coupling condition (50c), hence it is not canceling. To get a global energy identity, we need to modify equation (63) by left-multiplying it by $\widetilde{I}_{h,i}^{-1}$:

$$\widehat{M}_{h,i} D_{\Delta t}^2 U_{h,i}^n + K_{h,i} \{U_{h,i}^n\}_{1/4}^n - (-1)^i {}^t C_{h,i} \Pi_h^n = \widetilde{I}_{h,i}^{-1} S_{h,i}^n \quad (66)$$

Now the coupling condition (50c) appears after taking the scalar product with $(U_{h,i}^{n+1} - U_{h,i}^{n-1})/2\Delta t$ and summation:

$$\begin{aligned} \frac{\mathcal{E}_{01,4,h}^{n+1/2} - \mathcal{E}_{01,4,h}^{n-1/2}}{\Delta t} &= \Pi_h^n \cdot \left[C_{h,0} \frac{U_{h,0}^{n+1} - U_{h,0}^{n-1}}{2\Delta t} - C_{h,1} \frac{U_{h,1}^{n+1} - U_{h,1}^{n-1}}{2\Delta t} \right] \\ &\quad + \widetilde{I}_{h,0}^{-1} M_{h,0} S_{h,0}^n \cdot \frac{U_{h,0}^{n+1} - U_{h,0}^{n-1}}{2\Delta t} + \widetilde{I}_{h,1}^{-1} M_{h,1} S_{h,1}^n \cdot \frac{U_{h,1}^{n+1} - U_{h,1}^{n-1}}{2\Delta t} \end{aligned} \quad (67)$$

which leads to the expected result. \square

Proposition 7

The discrete energy (60) is positive if the matrices $\widehat{M}_{h,i}$ are positive for $i \in \{0, 1\}$.

Remark 4.2

Since $\widetilde{K}_{h,i} = \widetilde{I}_{h,i} K_{h,i}$, the non-negativity of $\widetilde{I}_{h,i}$ is a consequence of the non-negativity of $\widetilde{K}_{h,i}$. A problematic situation occurs when, for a given i , $\theta_i < 1/12$ and the time step Δt is exactly chosen as

$$\Delta t = \frac{1}{\sqrt{\left(\frac{1}{12} - \theta_i\right) \rho \left(K_{h,i} M_{h,i}^{-1}\right)}} \quad (68)$$

where ρ denotes the spectral radius. In this case, 0 is an eigenvalue of $\widetilde{I}_{h,i}$ which is therefore not invertible. It can be simply avoided by decreasing slightly the time step.

Remark 4.3

A sufficient condition for the positivity of the discrete energy (60) (i.e. positivity of $\widehat{M}_{h,i}$) is therefore the positivity of the energy (43) for each (θ_0, φ_0) and (θ_1, φ_1) -scheme on each subdomain, which is linked to the stability of the (θ_0, φ_0) and (θ_1, φ_1) -schemes on respectively domains Ω_0 and Ω_1 .

4.5. Stability

In this section we show the stability of scheme (50) in the case $\theta_i \geq 1/4$ and $\varphi_i \geq 1/4$.

Proposition 8

Suppose that the energy (60) is positive. Suppose also that $\theta_i \geq 1/4$ and $\varphi_i \geq 1/4$ for $i \in \{0, 1\}$. For any solution to (50) we have

$$\sqrt{\mathcal{E}_{01,4,h}^{n+1/2}} \leq \sqrt{\mathcal{E}_{01,4,h}^{1/2}} + \frac{\Delta t}{\sqrt{2}} \sum_{\ell=1}^n \left[\|S_{h,0}^\ell\|_{M_{h,0}} + \|S_{h,1}^\ell\|_{M_{h,1}} \right] \quad (69)$$

Proof

Using the energy identity (59) of proposition 6, we can write:

$$\begin{aligned} \left| \frac{\mathcal{E}_{01,4,h}^{n+1/2} - \mathcal{E}_{01,4,h}^{n-1/2}}{\Delta t} \right| &\leq \sum_{i=0}^1 \|S_{h,i}^n\|_{\widetilde{I}_{h,i}^{-1}M_{h,i}} \left\| \frac{U_{h,i}^{n+1} - U_{h,i}^{n-1}}{2\Delta t} \right\|_{\widetilde{I}_{h,i}^{-1}M_{h,i}} \\ &\leq \frac{1}{2} \sum_{i=0}^1 \|S_{h,i}^n\|_{\widetilde{I}_{h,i}^{-1}M_{h,i}} \left[\left\| \frac{U_{h,i}^{n+1} - U_{h,i}^n}{\Delta t} \right\|_{\widetilde{I}_{h,i}^{-1}\widetilde{M}_{h,i}} + \left\| \frac{U_{h,i}^n - U_{h,i}^{n-1}}{\Delta t} \right\|_{\widetilde{I}_{h,i}^{-1}\widetilde{M}_{h,i}} \right] \end{aligned} \quad (70)$$

Since $\widetilde{I}_{h,i}^{-1}$ are positive matrices and $\theta_i \geq 1/4$ and $\varphi_i \geq 1/4$, for any vector X ,

$$\widetilde{I}_{h,i}^{-1}M_{h,i}X \cdot X \leq \widetilde{I}_{h,i}^{-1}\widetilde{M}_{h,i}X \cdot X \quad (71)$$

From the definition of the energy (60) and since $K_{h,i}$ are positive matrices, we get

$$\left| \frac{\mathcal{E}_{01,4,h}^{n+1/2} - \mathcal{E}_{01,4,h}^{n-1/2}}{\Delta t} \right| \leq \frac{1}{2} \left(\sum_{i=0}^1 \|S_{h,i}^n\|_{\widetilde{I}_{h,i}^{-1}M_{h,i}} \right) \left[\sqrt{2\mathcal{E}_{01,4,h}^{n+1/2}} + \sqrt{2\mathcal{E}_{01,4,h}^{n-1/2}} \right] \quad (72)$$

We classically get

$$\frac{\sqrt{\mathcal{E}_{01,4,h}^{n+1/2}} - \sqrt{\mathcal{E}_{01,4,h}^{n-1/2}}}{\Delta t} \leq \frac{1}{\sqrt{2}} \sum_{i=0}^1 \|S_{h,i}^n\|_{\widetilde{I}_{h,i}^{-1}M_{h,i}} \quad (73)$$

which almost gives the expected result by summing from iterate $n = 1$ and recognizing a telescopic sum. However the proof is not over because $S_{h,i}^n$ is not estimated in the right norm. Since $\theta_i \geq 1/4$, we have for any vector X

$$M_{h,i}^{-1}\widetilde{I}_{h,i}X \cdot X \geq M_{h,i}^{-1}X \cdot X \quad (74)$$

By decomposing X on the basis of eigenvectors of $M_{h,i}^{-1/2}\widetilde{I}_{h,i}M_{h,i}^{1/2}$, it is easy to obtain that:

$$\widetilde{I}_{h,i}^{-1}M_{h,i}X \cdot X \leq M_{h,i}X \cdot X \quad (75)$$

Taking $X = S_{h,i}^n$ concludes our proof. \square

Proposition 9

Suppose that the energy (60) is positive. Suppose also that $\theta_i \geq 1/4$ and $\varphi_i \geq 1/4$ for $i \in \{0, 1\}$. For any solution to (50) we have

$$\begin{aligned} \|U_{h,i}^{n+1}\|_{M_{h,i}} &\leq \|U_{h,i}^0\|_{M_{h,i}} + t^{n+1} \eta(\theta_i) \sqrt{2} \sqrt{\mathcal{E}_{01,4,h}^{1/2}} \\ &\quad + \eta(\theta_i) \Delta t^2 \sum_{\ell=1}^n \sum_{k=1}^{\ell} \left[\|S_{h,0}^n\|_{M_{h,0}} + \|S_{h,0}^n\|_{M_{h,1}} \right] \end{aligned} \quad (76)$$

where

$$\eta(\theta) = 2 + \sqrt{1 + \left(\theta - \frac{1}{12}\right)} \quad (77)$$

Before showing this result, we need intermediate lemmas. Since the energy (60) involves a modified mass matrix, the expected estimate is not straightforward. We use the ideas introduced in article [15]. Let us introduce the family of eigenvectors $\{W_\ell\}_\ell$ and eigenvalues $0 \leq \mu_1 \leq \dots \leq \mu_\ell \leq \dots \leq \mu_{N_{h,i}}$ of $K_{h,i}$ in a $M_{h,i}$ -orthogonal basis :

$$\begin{cases} K_{h,i} W_\ell = \mu_\ell M_{h,i} W_\ell \\ M_{h,i} W_\ell \cdot W_k = \delta_{\ell,k}, \quad \forall (\ell, k) \end{cases} \quad (78)$$

We then introduce the so called “high-frequency” projector $P_{h,i}^\alpha$ such that

$$P_{h,i}^\alpha X = \sum_{\ell=L_\alpha}^{N_{h,i}} (M_{h,i} X \cdot W_\ell) W_\ell \quad (79)$$

where L_α is the smallest integer such that $\mu_{L_\alpha} \geq \alpha$. We will need the following estimates.

Lemma 1 (High frequency estimate)

For any vector X ,

$$\|P_{h,i}^\alpha X\|_{M_{h,i}}^2 \leq \frac{1}{\alpha} \|X\|_{K_{h,i}}^2 \quad (80)$$

Lemma 2 (Low frequency estimate)

For any vector X ,

$$\|(I_{h,i} - P_{h,i}^\alpha) X\|_{M_{h,i}}^2 \leq \left(1 + \Delta t^2 \left(\theta_i - \frac{1}{12}\right) \alpha\right) \|X\|_{\tilde{I}_{h,i}^{-1} M_{h,i}}^2 \quad (81)$$

Proof

The result of lemma 1 is shown in [15]. Let us now estimate the quantity

$$\tilde{I}_{h,i} M_{h,i} W_\ell = \left(M_{h,i} + \Delta t^2 \left(\theta_i - \frac{1}{12}\right) K_{h,i} \right) W_\ell \quad (82)$$

$$= \left(1 + \Delta t^2 \left(\theta_i - \frac{1}{12}\right) \mu_\ell \right) M_{h,i} W_\ell \quad (83)$$

Therefore, by inverting $\tilde{I}_{h,i}$

$$\tilde{I}_{h,i}^{-1} M_{h,i} W_\ell = \frac{1}{1 + \Delta t^2 \left(\theta_i - \frac{1}{12}\right) \mu_\ell} M_{h,i} W_\ell \quad (84)$$

We can now write

$$\begin{aligned}
\|X\|_{\tilde{I}_{h,i}^{-1}M_{h,i}}^2 &= \sum_{\ell=1}^{N_{h,i}} \sum_{j=1}^{N_{h,i}} (MX \cdot W_\ell) (MX \cdot W_j) \left(\tilde{I}_{h,i}^{-1} M_{h,i} W_\ell \cdot W_j \right) \\
&= \sum_{\ell=1}^{N_{h,i}} \frac{1}{1 + \Delta t^2 \left(\theta_i - \frac{1}{12} \right) \mu_\ell} (MX \cdot W_\ell)^2 \\
&\geq \sum_{\ell=1}^{L_\alpha-1} \frac{1}{1 + \Delta t^2 \left(\theta_i - \frac{1}{12} \right) \mu_\ell} (MX \cdot W_\ell)^2 \left(\text{since } 1 + \Delta t^2 \left(\theta_i - \frac{1}{12} \right) \mu_\ell \geq 0 \right) \\
&\geq \frac{1}{1 + \Delta t^2 \left(\theta_i - \frac{1}{12} \right) \alpha} \sum_{\ell=1}^{L_\alpha-1} (MX \cdot W_\ell)^2 \left(\text{since } \mu_\ell \leq \alpha \text{ for } \ell \leq L_\alpha - 1 \right) \\
&\geq \frac{1}{1 + \Delta t^2 \left(\theta_i - \frac{1}{12} \right) \alpha} \|(I_{h,i} - P_{h,i}^\alpha) X\|_{M_{h,i}}^2
\end{aligned} \tag{85}$$

which ends the proof of lemma 2 since $1 + \Delta t^2 \left(\theta_i - \frac{1}{12} \right) \alpha > 0$ (see remark 4.2). \square

Proof of proposition 9.

$$\|U_{h,i}^{n+1}\|_{M_{h,i}} \leq \underbrace{\|P_{h,i}^\alpha U_{h,i}^{n+1}\|_{M_{h,i}}}_{T_{HF}} + \underbrace{\|(I_{h,i} - P_{h,i}^\alpha) U_{h,i}^{n+1}\|_{M_{h,i}}}_{T_{LF}} \tag{86}$$

where HF and LF stand for high and low frequencies. Let us treat them differently. By triangular inequality, we have

$$\begin{cases} T_{HF} \leq \|P_{h,i}^\alpha U_{h,i}^n\|_{M_{h,i}} + 2 \left\| P_{h,i}^\alpha \frac{U_{h,i}^{n+1} + U_{h,i}^n}{2} \right\|_{M_{h,i}} \\ T_{LF} \leq \|(I_{h,i} - P_{h,i}^\alpha) U_{h,i}^n\|_{M_{h,i}} + \Delta t \left\| (I_{h,i} - P_{h,i}^\alpha) \frac{U_{h,i}^{n+1} - U_{h,i}^n}{\Delta t} \right\|_{M_{h,i}} \end{cases}$$

which give, using lemma (1) for high frequencies and lemma (2) for low frequencies:

$$\begin{cases} T_{HF} \leq \|P_{h,i}^\alpha U_{h,i}^n\|_{M_{h,i}} + \frac{2}{\sqrt{\alpha}} \left\| \frac{U_{h,i}^{n+1} + U_{h,i}^n}{2} \right\|_{K_{h,i}} \\ T_{LF} \leq \|(I_{h,i} - P_{h,i}^\alpha) U_{h,i}^n\|_{M_{h,i}} + \Delta t \sqrt{1 + \Delta t^2 \left(\theta_i - \frac{1}{12} \right) \alpha} \left\| \frac{U_{h,i}^{n+1} - U_{h,i}^n}{\Delta t} \right\|_{\tilde{I}_{h,i}^{-1}M_{h,i}} \end{cases}$$

In the last term of the first line, we recognize the discrete potential energy of domain Ω_i , which is smaller than the global energy. Similarly, the last term of the second line can easily (because $\theta_i \geq 1/4$ and $\varphi_i \geq 1/4$, see (71)) be bounded above with the discrete kinetic energy, which is also smaller than the total energy. We get:

$$\begin{cases} \|P_{h,i}^\alpha U_{h,i}^{n+1}\|_{M_{h,i}} \leq \|P_{h,i}^\alpha U_{h,i}^n\|_{M_{h,i}} + \frac{2}{\sqrt{\alpha}} \sqrt{2\mathcal{E}_{01,4,h}^{n+1/2}} \\ \|(I_{h,i} - P_{h,i}^\alpha) U_{h,i}^{n+1}\|_{M_{h,i}} \leq \|(I_{h,i} - P_{h,i}^\alpha) U_{h,i}^n\|_{M_{h,i}} + \Delta t \sqrt{1 + \Delta t^2 \left(\theta_i - \frac{1}{12} \right) \alpha} \sqrt{2\mathcal{E}_{01,4,h}^{n+1/2}} \end{cases}$$

After summing from iterate $n = 0$, we get

$$\left\{ \begin{array}{l} \|P_{h,i}^\alpha U_{h,i}^{n+1}\|_{M_{h,i}} \leq \|P_{h,i}^\alpha U_{h,i}^0\|_{M_{h,i}} + \frac{2\sqrt{2}}{\sqrt{\alpha}} \sum_{j=0}^n \sqrt{\mathcal{E}_{01,4,h}^{j+1/2}} \\ \|(I_{h,i} - P_{h,i}^\alpha) U_{h,i}^{n+1}\|_{M_{h,i}} \leq \|(I_{h,i} - P_{h,i}^\alpha) U_{h,i}^0\|_{M_{h,i}} + \Delta t \sqrt{2} \sqrt{1 + \Delta t^2 \left(\theta_i - \frac{1}{12}\right) \alpha} \sum_{j=0}^n \sqrt{\mathcal{E}_{01,4,h}^{j+1/2}} \end{array} \right.$$

We can now add these two contributions to bound equation (86).

$$\|U_{h,i}^{n+1}\|_{M_{h,i}} \leq \|P_{h,i}^\alpha U_{h,i}^0\|_{M_{h,i}} + \|(I_{h,i} - P_{h,i}^\alpha) U_{h,i}^0\|_{M_{h,i}} + \delta(\alpha) \Delta t \sqrt{2} \sum_{j=0}^n \sqrt{\mathcal{E}_{01,4,h}^{j+1/2}} \quad (89)$$

where $\delta(\alpha) = \frac{2}{\sqrt{\alpha} \Delta t} + \sqrt{1 + \Delta t^2 \left(\theta_i - \frac{1}{12}\right) \alpha}$. Notice that

$$\|P_{h,i}^\alpha X\|_{M_{h,i}} + \|(I_{h,i} - P_{h,i}^\alpha) X\|_{M_{h,i}} \leq \sqrt{2} \|X\|_{M_{h,i}} \quad (90)$$

We now use the energy estimate (69) of proposition 8.

$$\begin{aligned} \|U_{h,i}^{n+1}\|_{M_{h,i}} &\leq \sqrt{2} \|U_{h,i}^0\|_{M_{h,i}} + \delta(\alpha) \Delta t \sqrt{2} \sum_{j=0}^n \left[\sqrt{\mathcal{E}_{01,4,h}^{1/2}} + \frac{\Delta t}{\sqrt{2}} \sum_{\ell=1}^j \left[\|S_{h,0}^\ell\|_{M_{h,0}} + \|S_{h,1}^\ell\|_{M_{h,1}} \right] \right] \\ &\leq \sqrt{2} \|U_{h,i}^0\|_{M_{h,i}} + \delta(\alpha) t^{n+1} \sqrt{2} \sqrt{\mathcal{E}_{01,4,h}^{1/2}} + \delta(\alpha) \Delta t^2 \sum_{j=0}^n \sum_{\ell=1}^j \left[\|S_{h,0}^\ell\|_{M_{h,0}} + \|S_{h,1}^\ell\|_{M_{h,1}} \right] \end{aligned}$$

Notice that the choice

$$\alpha = \frac{1}{\Delta t^2} \Rightarrow \delta(\alpha) = 2 + \sqrt{1 + \left(\theta_i - \frac{1}{12}\right)} := \eta(\theta_i) \quad (91)$$

ensures the independence of the constant with respect to Δt . \square

Remark 4.4

The proof of an energy identity and the resulting estimate on the solution has been given here in the case where $\theta_i \geq 1/4$ and $\varphi_i \geq 1/4$, $i \in \{0, 1\}$. The other situation raises non standard issues (because of the unusual form of the energy) and will be the object of a forthcoming study. More precisely, equations (71) and (75) are no longer true.

4.6. Fourth order consistency

We are now interested in the consistency of (50) with (7). To this purpose, and as before, we define the errors

$$e_{h,i}^n = U_{h,i}^n - \tilde{U}_{h,i}(t^n), \quad e_{h,\lambda}^n = \left(\Pi_h^n - \tilde{\Lambda}_h(t^n) - \frac{\Delta t^2}{12} \frac{d^2}{dt^2} \tilde{\Lambda}_h(t^n) \right)$$

Proposition 10

The error $(e_{h,0}, e_{h,1}, e_{h,\lambda})$ is solution to the system of equations:

$$\begin{cases} M_{h,0} D_{\Delta t}^2 e_{h,0}^n + K_{h,0} \{e_{h,0}\}_{\theta_0}^n - {}^t C_{h,0} e_{h,\lambda}^n = \\ \quad + \Delta t^2 \left(\theta_0 - \frac{1}{12} \right) K_{h,0} M_{h,0}^{-1} [-K_{h,0} \{e_{h,0}\}_{\varphi_0}^n + {}^t C_{h,0} e_{h,\lambda}^n] + \mathcal{O}(\Delta t^4) \end{cases} \quad (92a)$$

$$\begin{cases} M_{h,1} D_{\Delta t}^2 e_{h,1}^n + K_{h,1} \{e_{h,1}\}_{\theta_1}^n + {}^t C_{h,1} e_{h,\lambda}^n = \\ \quad + \Delta t^2 \left(\theta_1 - \frac{1}{12} \right) K_{h,1} M_{h,1}^{-1} [-K_{h,1} \{e_{h,1}\}_{\varphi_1}^n + {}^t C_{h,1} e_{h,\lambda}^n] + \mathcal{O}(\Delta t^4) \end{cases} \quad (92b)$$

$$\begin{cases} C_{h,0} \frac{e_{h,0}^{n+1} - e_{h,0}^{n-1}}{2\Delta t} - C_{h,1} \frac{e_{h,1}^{n+1} - e_{h,1}^{n-1}}{2\Delta t} = 0 \end{cases} \quad (92c)$$

This system of equations on the errors shows that scheme (50) is consistent with the semi discrete system (7) up to order four.

Proof

We first define the discrete operator acting on a series of vectors X^n , $n \in \mathbb{N}$:

$$\mathcal{L}_0(X^n) = M_{h,0} D_{\Delta t}^2 X^n + K_{h,0} \{X^n\}_{\theta_0}^n + \Delta t^2 \left(\theta_0 - \frac{1}{12} \right) K_{h,0} M_{h,0}^{-1} K_{h,0} \{X^n\}_{\varphi_0}^n \quad (93)$$

And we evaluate $\mathcal{L}_0(e_{h,0}^n)$ which by linearity is

$$\mathcal{L}_0(e_{h,0}^n) = \mathcal{L}_0(U_{h,0}^n) - \mathcal{L}_0(\tilde{U}_{h,0}(t^n)) \quad (94)$$

For the first term, we use equation (50a) to get

$$\mathcal{L}_0(U_{h,0}^n) = {}^t C_{h,0} \Pi_h^n + M_{h,0} S_{h,0}^n + \Delta t^2 \left(\theta_0 - \frac{1}{12} \right) K_{h,0} M_{h,0}^{-1} {}^t C_{h,0} \Pi_h^n \quad (95)$$

and for the second term, we use proposition 1 and we get, using again the semi discrete equation (7):

$$\begin{aligned} \mathcal{L}_0(\tilde{U}_{h,0}(t^n)) &= {}^t C_{h,0} \tilde{\Lambda}_h(t^n) + M_{h,0} \tilde{S}_{h,0}(t^n) + \Delta t^2 {}^t C_{h,0} \frac{d^2 \tilde{\Lambda}_h}{dt^2}(t^n) + \Delta t^2 M_{h,0} \frac{d^2 \tilde{S}_{h,0}}{dt^2}(t^n) \\ &\quad + \Delta t^2 \left(\theta_0 - \frac{1}{12} \right) K_{h,0} M_{h,0}^{-1} [{}^t C_{h,0} \tilde{\Lambda}_h(t^n) + M_{h,0} \tilde{S}_{h,0}(t^n)] + \mathcal{O}(\Delta t^4) \end{aligned} \quad (96)$$

According to the definition of the discrete source term (41), we have:

$$\begin{aligned} \mathcal{L}_0(e_{h,0}^n) &= {}^t C_{h,0} \left[\Pi_h^n - \tilde{\Lambda}_h(t^n) - \Delta t^2 \frac{d^2 \tilde{\Lambda}_h}{dt^2}(t^n) \right] \\ &\quad + \Delta t^2 \left(\theta_0 - \frac{1}{12} \right) K_{h,0} M_{h,0}^{-1} {}^t C_{h,0} [\Pi_h^n - \tilde{\Lambda}_h(t^n)] + \mathcal{O}(\Delta t^4) \end{aligned} \quad (97)$$

We obtain equation (92a) by inserting $-\Delta t^2 \frac{d^2 \tilde{\Lambda}_h}{dt^2}(t^n)$ in the second bracket, which is consistent since it is a $\mathcal{O}(\Delta t^4)$ term. We proceed similarly for the second domain to obtain (92b). Finally, to obtain (92c), we can apply the same arguments as in the proof of proposition 5. \square

Remark 4.5 (Splitting)

A valid alternative in the case of conformal meshes is to perform the modified equation technique

on the splitted equation (31). The consistency error reads:

$$\sum_{m=1}^{\infty} \Delta t^{2m} \left(\frac{2}{(2m+2)!} (M_{h,0} + M_{h,1}) \frac{d^2}{dt^2} + \frac{2\theta_0}{(2m)!} K_{h,0} + \frac{2\theta_1}{(2m)!} K_{h,1} \right) \frac{d^{2m}}{dt^{2m}} \tilde{U}_h(t^n)$$

Using equation (31), we can replace $(M_{h,0} + M_{h,1}) \frac{d^2}{dt^2}$ by $-K_{h,0} - K_{h,1}$ and truncating the series at $m = 1$, the error writes:

$$-\Delta t^2 \left[\left(\theta_0 - \frac{1}{12} \right) K_{h,0} + \left(\theta_1 - \frac{1}{12} \right) K_{h,1} \right] (M_{h,0} + M_{h,1})^{-1} (K_{h,0} + K_{h,1}) \tilde{U}_h(t^n) + \mathcal{O}(\Delta t^4)$$

Hence the possible implicit fourth order scheme:

$$\begin{aligned} & M_{h,0} D_{\Delta t}^2 U_h^n + M_{h,1} D_{\Delta t}^2 U_h^n + K_{h,0} \{U\}_{\theta_0}^n + K_{h,1} \{U\}_{\theta_1}^n \\ & + \Delta t^2 \left(\theta_0 - \frac{1}{12} \right) K_{h,0} M_h^{-1} K_{h,0} \{U_h\}_{\varphi_0}^n + \Delta t^2 \left(\theta_1 - \frac{1}{12} \right) K_{h,1} M_h^{-1} K_{h,1} \{U_h\}_{\varphi_1}^n \\ & + \Delta t^2 \left(\theta_0 - \frac{1}{12} \right) K_{h,0} M_h^{-1} K_{h,1} \{U_h\}_{\psi_0}^n + \Delta t^2 \left(\theta_1 - \frac{1}{12} \right) K_{h,1} M_h^{-1} K_{h,0} \{U_h\}_{\psi_1}^n = 0 \end{aligned}$$

Obtaining symmetric operators imposes the choice $\theta_0 = \theta_1$ and $\psi_0 = \psi_1$. It therefore prevents any explicit / implicit coupling and looses the interest of such schemes. Dealing with non symmetric operators may be possible but stability is, to our knowledge, not granted by usual energy estimates.

4.7. Numerical illustration

In this section we present numerical illustrations obtained with scheme (50) in 1D and 2D along with high order spectral finite elements using the mass lumping method. First, we consider the same illustrative 1D scalar test case as in section 3.7, and we perform our hybrid fourth order scheme with $(\theta_0, \varphi_0) = (0, 0)$ on the left half of the domain, and $(\theta_1, \varphi_1) = (1/4, 1/4)$ on the right part. The time step is chosen the same as before, i.e.

$$\Delta t = 5.2 \times 10^{-3} \text{ sec.} \quad (98)$$

In Fig. 4 are displayed snapshots of the solution at times $t = 0$, $t = 0.25$ and $t = 0.5$ sec in blue circles, along with the analytical solution in solid red line. The maximal value of the relative L2 error with the analytical solution along time is 4.49×10^{-2} . Numerical dispersion is clearly smaller than in figure 1. The discrete energy of the numerical solution is computed for each time step following formula (60). The relative total energy deviation is of about the machine precision (10^{-14}). The total energy is plotted in Fig. 5 along with the energies of each sub-domain in plain curves, and compared to the naive energy coming from formula (43) (dashed curves). One can see that the naive total energy is not preserved when the wave crosses the interface.

In figure 6 are displayed a series of spatio-temporal convergence curves obtained with similar numerical experiments than those in section 3.7. The second order hybrid scheme (explicit / $1/4$)-scheme is represented in blue circles using the same discretization parameters as those for Fig. 3 (both the space and time steps tend to zero in this curve, and we use respectively third, sixth and eighth order finite elements). The fourth order hybrid scheme (explicit / $(1/4, 1/4)$)-scheme is represented in red diamonds using the same spatial meshes, but a time step Δt equal to the largest Δt such that $\tilde{M}_{h,i}$ and $\tilde{K}_{h,i}$ defined in Eq. (62b) and (64a) are positive (hence ensuring stability). Finally, the green triangle curve is obtained similarly to the red diamonds curve, using the same discretization parameters, but neglecting the last term of Eq. (50a) and the last term of Eq. (50b). This corresponds to a naive approach where two fourth order numerical schemes are interfaced using a coupling condition adapted to second order schemes. The fourth order hybrid scheme (explicit / $(1/4, 1/4)$)-scheme exhibits the expected fourth order rate of convergence. However, a first order convergence rate is observed for the “naive” coupling, where a second order convergence rate would have been the intuitive guess. This emphasizes the necessity of adequately tackling the

transmission conditions when using high order time stepping in the volumic regions, otherwise the global precision can even be deteriorated compared to using lower order time stepping in the volumic regions.

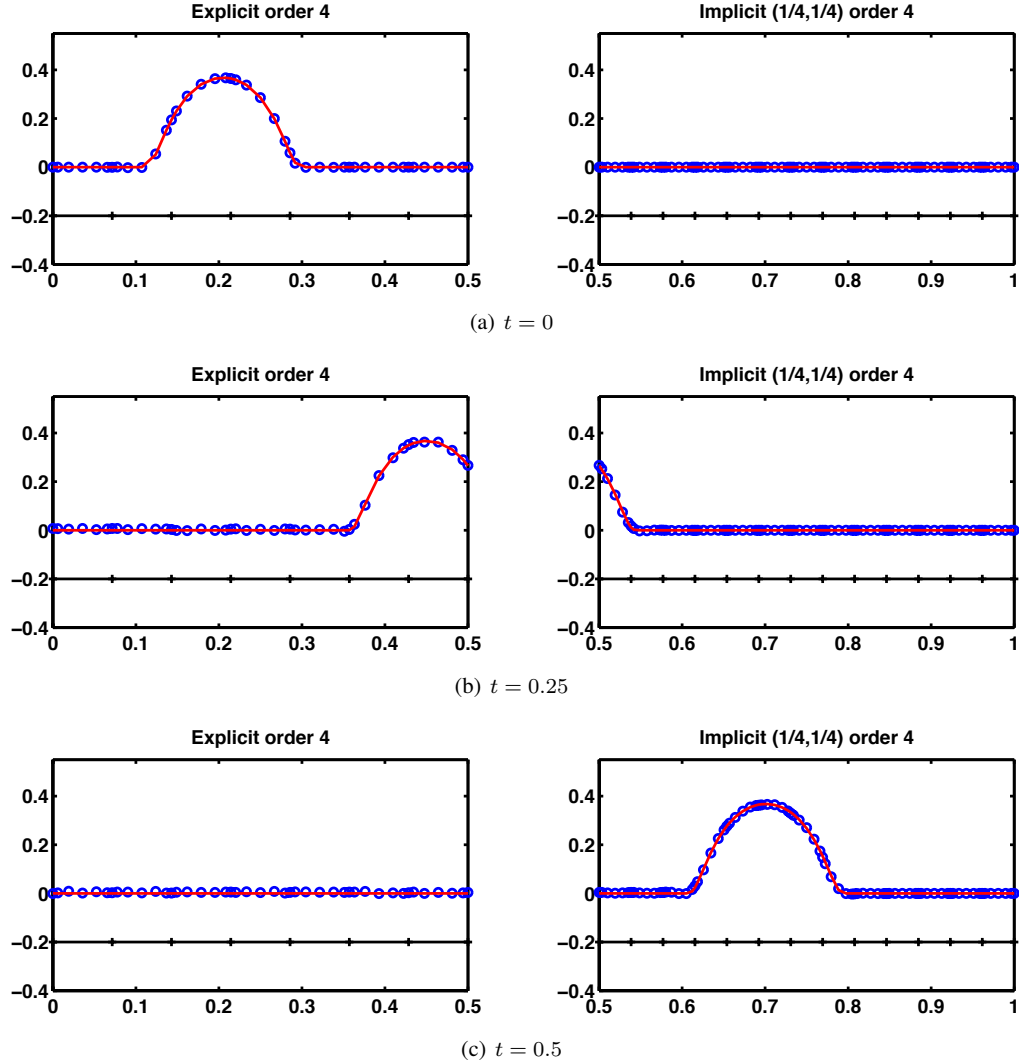


Figure 4. Snapshots of the analytical solution (in red solid line) and numerical solution (in blue circles). In black is displayed the mesh on each part of the domain.

Let us now consider the following 2D scalar acoustic experiment. The domain is composed of two unit square regions where the acoustic wave propagates at 1 m/s surrounding a small rectangular layer of size 0.1×1 m where the acoustic wave velocity is diagonally anisotropic: $c_x = 50$ m/s and $c_y = 5$ m/s. Initial conditions are zero and a source term is considered:

$$S(x, y, t) = \frac{-1000}{t - \tau} \mathbb{1}_{t \in [0, \tau]} e^{-\frac{\tau/2}{|t - \tau/2| - \tau/2}} e^{-2000((x - x_0)^2 + (y - y_0)^2)} \quad (99)$$

where (x_0, y_0) is the middle point of the right unit square, and $\tau = 0.1$ sec. Homogeneous Neumann boundary conditions are imposed all around the domain. The spatial discretization is done with

mass lumped sixth order spectral finite elements. The unit squares are meshed by 20×20 squared elements and the layer is meshed with 4×20 rectangular elements. The final time of simulation is

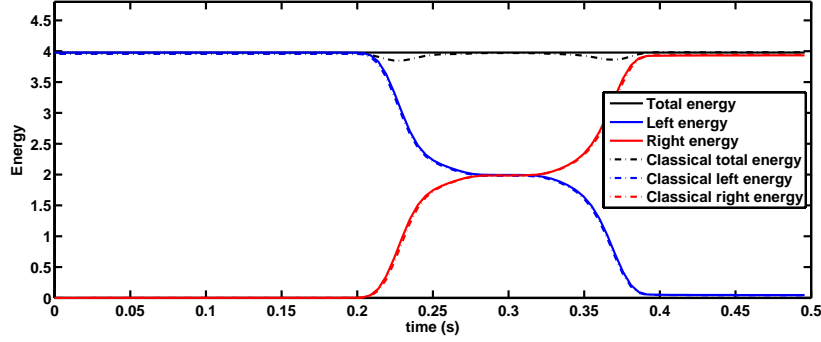
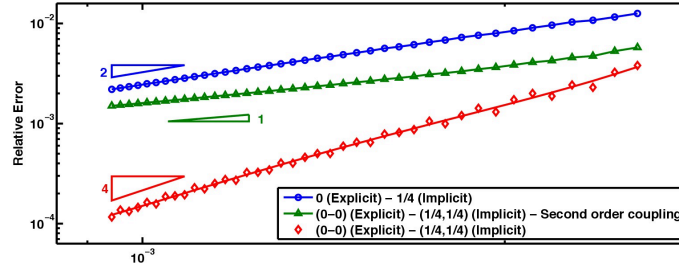
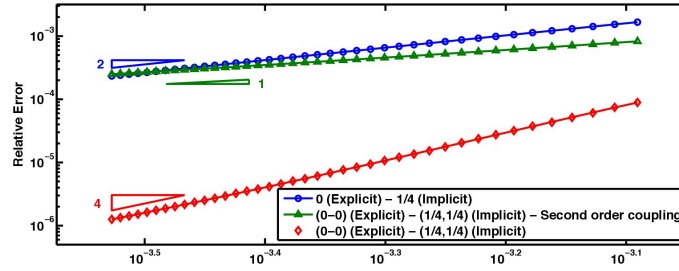


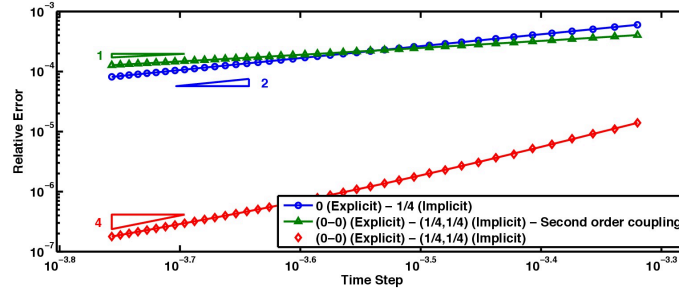
Figure 5. Total energy evolution



(a) Third Order Finite Elements



(b) Sixth Order Finite Elements



(c) Eighth Order Finite Elements

Figure 6. Maximal relative L2 error with the analytical solution along time for schemes (15) and (50).

2.8 sec. Different time schemes are considered. The subscripts ℓ, m, r are used to denote respectively the left square, middle layer and right square.

Scheme A: Second order hybrid scheme with $\theta_\ell = 0$, $\theta_m = 0$ and $\theta_r = 0$. The time step is chosen close to its largest possible value which is imposed by the explicit scheme in the middle layer:

$$\Delta t_A = 3.2 \times 10^{-5} \text{ sec.} \quad (100)$$

The total computational cpu time is 152.7 sec.

Scheme B: Second order hybrid scheme with $\theta_\ell = 0$, $\theta_m = 1/4$ and $\theta_r = 0$. The stability condition is $\Delta t \leq 2.59 \times 10^{-3}$ sec. We choose

$$\Delta t_B = 70 \times \Delta t_A = 2.24 \times 10^{-3} \text{ sec.} \quad (101)$$

The total computational cpu time is 3.4 sec.

Scheme C: Fourth order hybrid scheme with $(\theta_\ell, \varphi_\ell) = (0, 0)$, $(\theta_m, \varphi_m) = (1/4, 1/4)$ and $(\theta_r, \varphi_r) = (0, 0)$. The time step must respect the stability condition $\Delta t \leq 4.47 \times 10^{-3}$ sec. We choose

$$\Delta t_C = \Delta t_A \quad (102)$$

The total computational cpu time is 492.1 sec.

Scheme D: Fourth order hybrid scheme with $(\theta_\ell, \varphi_\ell) = (0, 0)$, $(\theta_m, \varphi_m) = (1/4, 1/4)$ and $(\theta_r, \varphi_r) = (0, 0)$. The time step is chosen close to its largest allowed value

$$\Delta t_D = 125 \times \Delta t_A = 4 \times 10^{-3} \text{ sec.} \quad (103)$$

The total computational cpu time is 4.0 sec.

In Fig. 7 we plot with respect to time the relative discrete H1-error computed in each domain (computed with the discrete norm $\|\cdot\|_{M_{h,i}+K_{h,i}}$) between the solutions obtained with schemes **B**, **C**, **D** and the reference solution (which is obtained using Scheme **A**). A good agreement is observed between both solutions computed with the small time step Δt_A . This experimentally confirms that they converge to the same solution as expected theoretically. The solution obtained with scheme **B** rapidly deviates from the reference solution when time increases. This is due to the strong numerical dispersion of this second order accurate scheme. We see that scheme **D**, for a small computational overhead compared to scheme **B** (18 % more costly), leads to a significantly smaller error on the solution, which stays relatively constant when time increases. In Fig. 8 are displayed the snapshots of the numerical solution obtained for scheme **D**. The pulse crosses the small layer at a very high velocity and multiple reflections are visible. The relative total energy deviation with respect to time obtained using formula (60) is of about the machine precision (10^{-14}), in accordance with theoretical expectations. The energy evolution is displayed in Fig. 9 in the different subdomains as well as the total energy. The energies are computed either using formula (60) (solid lines) or the classical energy given by formula (43) (in dashed lines). We see that the latter is not exactly preserved, especially when the wave crosses an interface.

Finally to illustrate that our method can be used in more complex situations than the scalar acoustic wave equation (1), we present in Fig. 10, snapshots of a 2-dimensional linear isotropic elastodynamics simulation in the same domain as in the previous configuration. The unknown is a displacement field $\mathbf{u} = {}^t(u_1, u_2)$, the applied source term is ${}^t(0, S(x, y, t))$, where S is defined in Eq. (99). The density and the Young's modulus are set to 1 in all domains, the left and right squares have a Poisson's ratio of 0.25, the middle layer represents a very soft medium and has a Poisson's ratio of 0.499. The same discretization parameters as for the scalar case are used (mesh size, time step, order of the finite elements). The same conclusion in term of performances has been drawn.

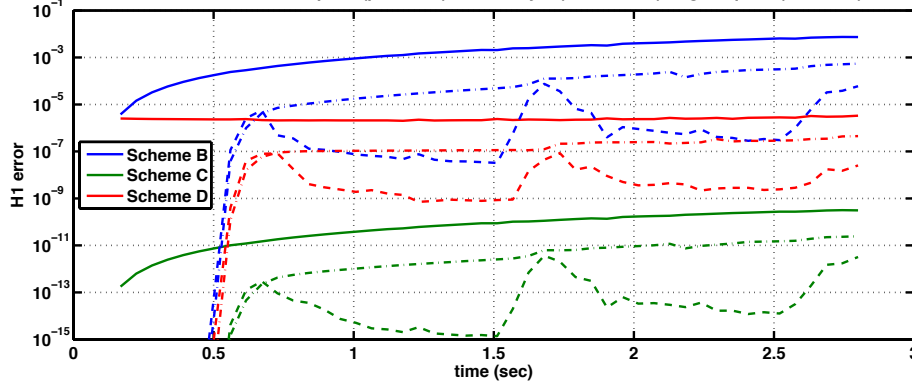


Figure 7. Relative error, left square (point line), middle layer (dashed line), right square, (solid line), for schemes **B**, **C**, **D** with the solution obtained using scheme **A**.

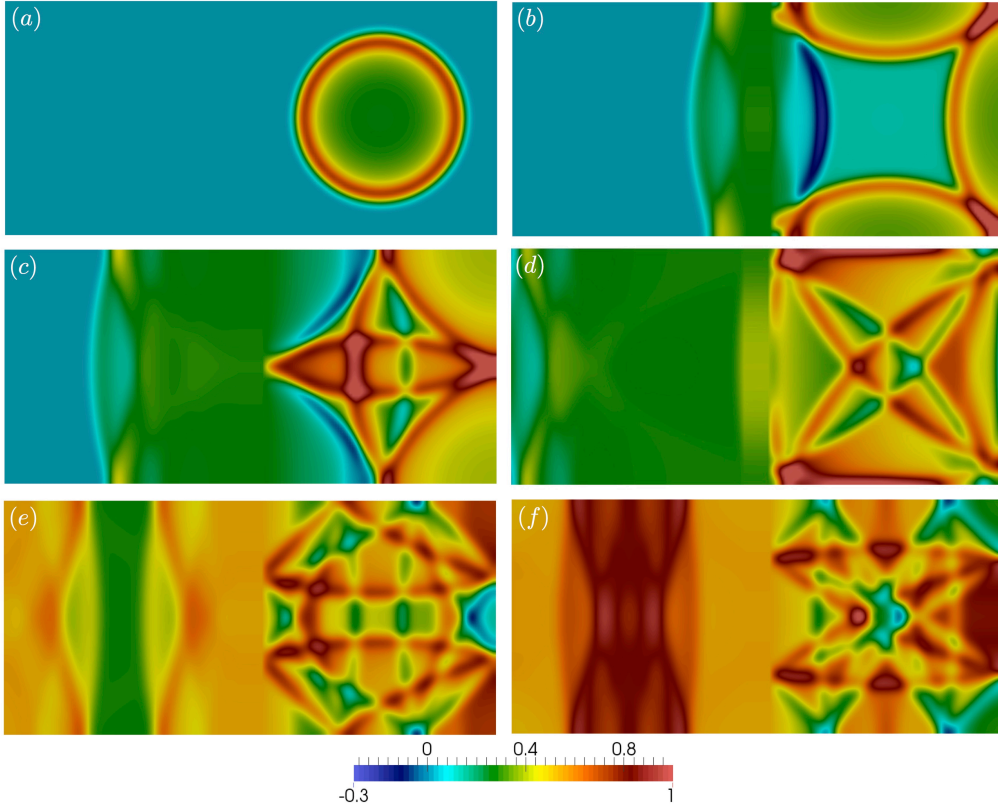


Figure 8. Snapshots of the numerical solution using scheme **D** (a) $t = 0.448$ sec. (b) $t = 0.840$ sec. (c) $t = 1.232$ sec. (d) $t = 1.624$ sec. (e) $t = 2.016$ sec. (f) $t = 2.408$ sec.

5. CONCLUSION AND PROSPECTS

In this paper we have designed a general family of fourth order time schemes that couple, on different regions of the computational domain, implicit schemes designed in [15] that depend on parameters (θ, φ) . The value of these parameters are different on each region of the domain. A specific choice of the parameters' set provides locally implicit fourth order time schemes. Although in this method, the time step is constant and the same in all the domain, it can be seen as an alternative to local time stepping, since the presence of local heterogeneities do not penalize the

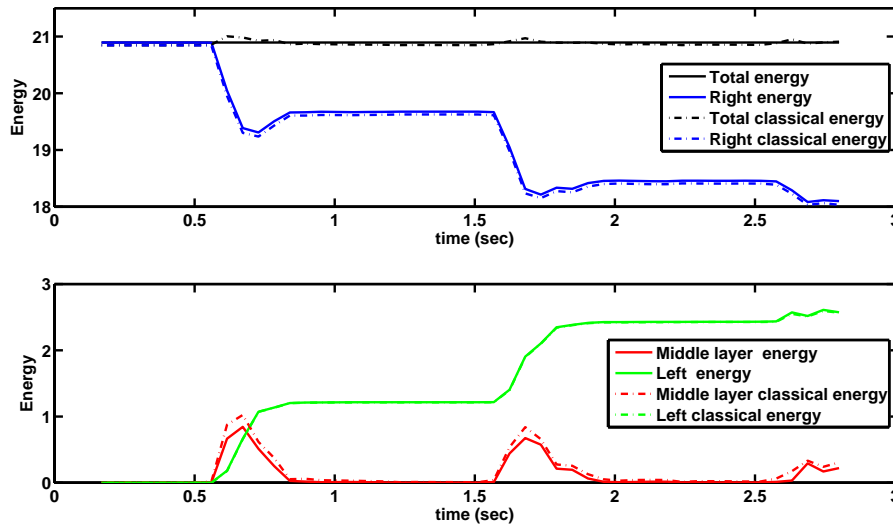


Figure 9. Energy evolution in each part of the domain for the solution of scheme D.

global efficiency of the numerical scheme. Non standard energy identities can be derived. Stability in the natural mass matrix norm has been proven for a sub-family of these schemes: $\theta \geq 1/4$ and $\varphi \geq 1/4$. The proof of stability in the mass matrix norm requires thorough analysis for θ or $\varphi \leq 1/4$, as mentioned in remark 4.4. Another difficult point is the theoretical proof of space / time convergence because the provided analysis does not guaranty conventional behavior of the solution for coupled values of the space and time discretization steps, although numerical results illustrate the good behavior of our method. Finally, a first interesting extension of this work concerns the study of elasto-acoustic wave coupling at an interface. Indeed such a configuration enters the same mathematical framework since the wave equations exhibit similar mathematical properties, however the coupling condition is different. Another thrilling prospect would be to ensure a stable fourth order coupling between the presented schemes and a non energy-based numerical fourth order numerical time scheme such as Runge Kutta 4. This possibility would enable us to provide high order in time stable numerical schemes for linear and nonlinear wave coupling at an interface which presents a great interest in realistic simulations.

REFERENCES

1. P. G. Ciarlet, The Finite Element Method for Elliptic Problems, *Classics in Applied Mathematics*, SIAM, 2002.
2. G. Cohen, Higher-order numerical methods for transient wave equations, *Springer-Verlag*, 2001.
3. Y. Maday, and A T Patera, Spectral element methods for the incompressible Navier-Stokes equations, *State-of-the-art surveys on computational mechanics*, American Society of Mechanical Engineers, 1989.
4. Komatitsch, D and Tromp, J Introduction to the spectral element method for three-dimensional seismic wave propagation, *Geophysical Journal International*, vol 139(3), pp 806–822, 2002.
5. G Derveaux and A Chaigne and P Joly and E Bécache, Time-domain simulation of a guitar: Model and method, *The Journal of the Acoustical Society of America*, vol. 114(6), pp 3368–3384, 2003.
6. L. Krivodonova An efficient local timestepping scheme for solution of nonlinear conservation laws. *Journal of Computational Physics*, vol. 229(22), pp 8537–8551, 2010.
7. A. Kanevsky, M. Carpenter, D. Gottlieb, J. Hesthaven Application of implicitexplicit high order RungeKutta methods to discontinuous Galerkin schemes *Journal of Computational Physics*, vol. 225(2), pp 1753–1781, 2007.
8. M. Dumbser, M. Kser and E. F. Toro An Arbitrary High Order Discontinuous Galerkin Method for Elastic Waves on Unstructured Meshes V: Local Time Stepping and p-Adaptivity *Geophysical Journal International*, vol. 171(2), pp 695–717, 2007.
9. F. Lorcher, G. Gassner, C.D. Munz A discontinuous Galerkin scheme based on a spacetime expansion. I. Inviscid compressible flow in one space dimension *Journal of Computational Physics* vol. 32(2), pp 175–199, 2007.
10. A. Taube, M. Dumbser, C.D. Munz, R. Schneider A high-order discontinuous Galerkin method with time-accurate local time stepping for the Maxwell equations *International Journal of Numerical Modelling: Electronic*

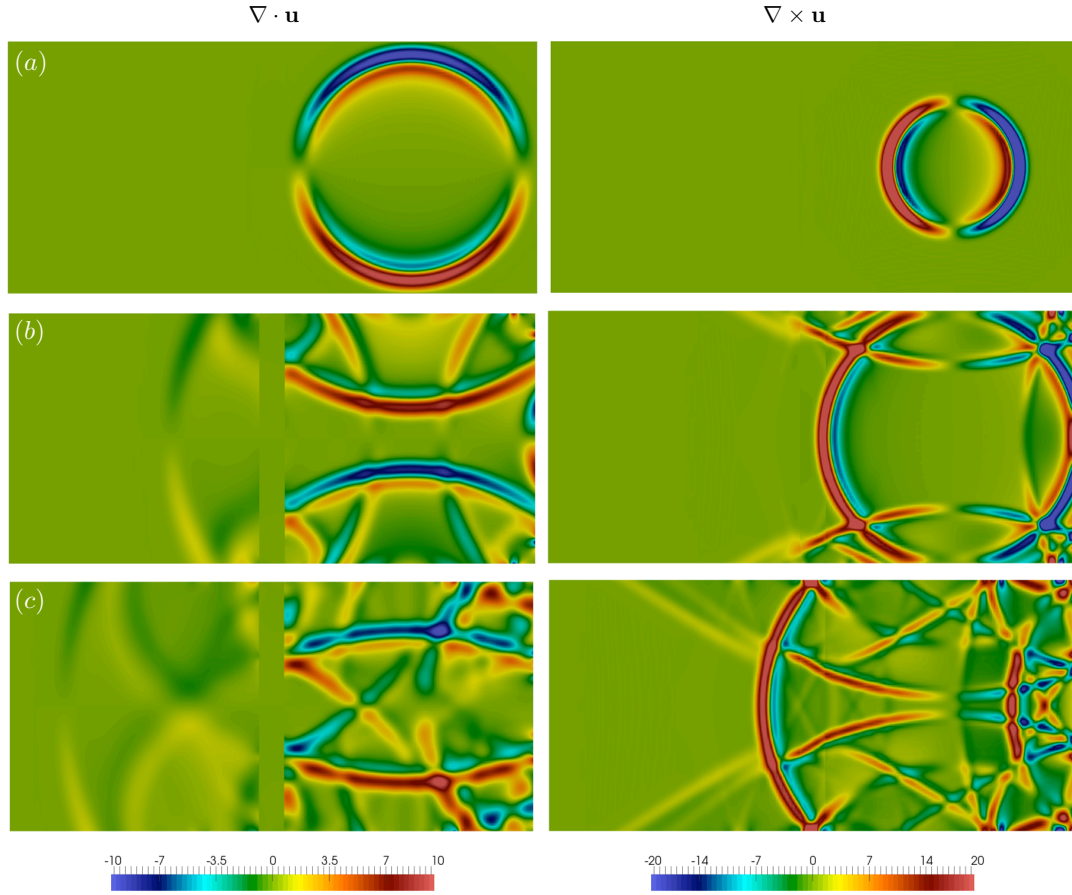


Figure 10. Snapshots of the numerical solution using scheme **D** (a) $t = 0.448$ sec. (b) $t = 0.840$ sec. (c) $t = 1.232$ sec. Figures on the left represent the divergence of the displacement field \mathbf{u} , figures on the right represent the 2-dimensional rotational of the displacement field \mathbf{u} .

- Networks, Devices And Fields*, vol. 22(1), pp 77–103, 2009.
11. F. Collino, T. Fouquet, P. Joly, A conservative space-time mesh refinement method for the 1-d wave equation. Part I: Construction, *Numerische Mathematik*, vol. 95 (2), pp 197–221, 2003.
 12. F. Collino, T. Fouquet, P. Joly, A conservative space-time mesh refinement method for the 1-D wave equation. II. Analysis, *Numerische Mathematik*, vol. 95 (2) pp 223–251, 2003.
 13. E. Becache, P. Joly, J. Rodríguez, Space-time mesh refinement for elastodynamics. Numerical results *Computer Methods in Applied Mechanics and Engineering*, vol. 194 (2-5), pp 355–366, 2005.
 14. J. Diaz, M. Grote, Energy conserving explicit local time-stepping for second-order wave equations, *SIAM Journal on Scientific Computing*, vol. 31 (3), pp 1985–2014, 2009.
 15. J. Chabassier, S. Imperiale. Introduction and study of fourth order theta schemes for linear wave equations, *Journal of Computational and Applied Mathematics*, vol. 245, pp 194–212, 2012.
 16. T. Rylander, Stability of Explicit–Implicit Hybrid Time-Stepping Schemes for Maxwell’s Equations, *Journal of Computational Physics*, vol. 179 (2), pp 426–438, 2002.
 17. V. Doleana, H. Fahs, L. Fezoui, S. Lanteri. Locally implicit discontinuous Galerkin method for time domain electromagnetics, *Journal of Computational Physics*, vol. 229(2), pp 512–526, 2010.
 18. S. Descombes, S. Lanteri, L. Moya, Locally implicit time integration strategies in a discontinuous Galerkin method for Maxwell’s equations, *Journal of Scientific Computing*, vol 56(1), pp 190–218, 2013.
 19. C. Baldassari, H. Barucq, H. Calandra, B. Denel, J. Diaz Performance Analysis of a High-Order Discontinuous Galerkin Method. Application to the Reverse Time Migration *Communications in Computational Physics*, vol. 11(2), pp 660–673, 2012.
 20. Y. Maday, C. Mavriplis, A. T. Patera, Nonconforming mortar element methods - Application to spectral discretizations in Domain decomposition methods, *SIAM Philadelphia*, pp 392–418, 1989.
 21. P. Joly, J. Rodriguez Effective computational methods for wave propagation. Chap 13 : Space time mesh refinement methods, *Chapman and Hall/CRC*, 2008.
 22. F. Brezzi, . Fortin Mixed and Hybrid Finite Element Methods, *Springer Series in Computational Mathematics*, vol. 15, 1991.
 23. G. Cohen, P. Joly, J. E. Roberts, N. Tordjman, Higher-order triangular finite elements with mass lumping for the

- wave equation, SIAM, *J. Numer. Anal.*, vol. 38 (6), pp 2047–2078, 2001.
24. M. J. S. Chin-Joe-Kong, W. A. Mulder, M. Van Veldhuizen, Higher-order triangular and tetrahedral finite elements with mass lumping for solving the wave equation. *Journal of Engineering Mathematics*, vol. 35, pp 405–426, 1999.
 25. R. Dautray, J.L. Lions, C. Bardos, M. Cessenat, P. Lascaux, A. Kavenoky, B. Mercier, O. Pironneau, B. Scheurer, and R. Sentis. *Mathematical analysis and numerical methods for science and technology - vol. 6.* Springer, 2000.
 26. J. Chabassier, S. Imperiale. Stability and dispersion analysis of improved time discretization for simply supported prestressed Timoshenko systems. Application to the stiff piano string, *Wave Motion*, vol. 50, pp 456–480, 2013.